The Astronomy and Astrophysics Review (2018) 26:4
https://doi.org/10.1007/s00159-018-0109-x

REVIEW ARTICLE

The interstellar and circumnuclear medium of active nuclei traced by H I 21 cm absorption

Raffaella Morganti[1,2] · **Tom Oosterloo**[1,2]

Received: 23 April 2018 / Published online: 17 July 2018

Abstract

This review summarises what we have learnt in the last two decades based on H I 21 cm absorption observations about the cold interstellar medium (ISM) in the central regions of active galaxies and about the interplay between this gas and the active nucleus (AGN). H I absorption is a powerful tracer on all scales, from the parsec-scales close to the central black hole to structures of many tens of kpc tracing interactions and mergers of galaxies. Given the strong radio continuum emission often associated with the central activity, H I absorption observations can be used to study the H I near an active nucleus out to much higher redshifts than is possible using H I emission. In this way, H I absorption has been used to characterise in detail the general ISM in active galaxies, to trace the fuelling of radio-loud AGN, to study the feedback occurring between the energy released by the active nucleus and the ISM, and the impact of such interactions on the evolution of galaxies and of their AGN. In the last two decades, significant progress has been made in all these areas. It is now well established that many radio loud AGN are surrounded by small, regularly rotating gas disks that contain a significant fraction of H I. The structure of these disks has been traced down to parsec scales by very long baseline interferometry observations. Some groups of objects, and in particular young and recently restarted radio galaxies, appear to have a particularly high detection rate of H I. This is interesting in connection with the evolution of these AGN and their impact on the surrounding ISM. This is further confirmed by an important discovery, made thanks to technical upgrades of radio telescopes, namely the presence of fast, AGN-driven outflows of cold gas which give a direct view of the impact of the energy released by AGN on the evolution of galaxies (AGN feedback). In addition, evidence has been collected that clouds of cold gas can play a role in fuelling the nuclear activity. This review ends by briefly describing the upcoming large, blind H I absorption surveys planned for the new radio telescopes which will soon become operational. These surveys will allow to significantly expand existing work, but will also allow to explore new topics, in particular, the evolution of the cold ISM in AGN.

Keywords Galaxies: active · ISM: jets and outflow · Radio lines: galaxies

Extended author information available on the last page of the article

1 Introduction

As is well known, hydrogen is the most common element in the Universe and it is observed in structures which span from the largest cosmological scales to the small, pc-scale of the centres of galaxies. Depending on the physical conditions, hydrogen occurs in all possible phases, ranging from atomic and molecular gas in the colder interstellar medium (ISM; with temperatures up to a few thousand kelvin), warm ionised gas (with temperatures of the order of 10^4 K) in the warmer ISM and in intragalactic space, to very hot ionised gas (with temperatures of 10^6 K or even higher) in the circum-galactic medium around galaxies, and in groups and clusters of galaxies (e.g. Wolfire 2010). Obviously, using different types of observations of the different phases of hydrogen, a very large variety of astronomical phenomena can be studied.

In this context, since the prediction of the hyperfine transition of atomic hydrogen (H I) at a rest-frame frequency of 1.4204 GHz, or wavelength $\lambda = 21.1$ cm, by Henk van de Hulst in 1944 and the successive first detections of the H I line in 1951 by Ewen and Purcell in the USA (Ewen and Purcell 1951), Muller and Oort in the Netherlands (Muller and Oort 1951), and Christiansen and Hindman in Australia (Christiansen and Hindman 1952), studies based on radio observations of atomic hydrogen have indeed made very significant contributions to the understanding of a very wide range of astronomical problems.

From the start, studies using the H I line in emission have played a key role in the understanding of the kinematics, structure and evolution of our own Milky Way (Oort et al. 1958), as well as of other galaxies in general. In particular, such work has played a central role in uncovering the properties of dark matter in galaxies, and in showing the importance for the evolution of galaxies of gas accretion/circulation as well of interactions between galaxies with their environment (see Sanders 2014 and Sancisi et al. 2008 for reviews of these topics and Giovanelli and Haynes 2015 for a review on recent H I emission surveys). The relevance of H I studies for understanding the formation and evolution of galaxies, and even for studying the evolution of the Universe as a whole (e.g. the Epoch of Reionisation), is still very high and is one of the main scientific drivers for the construction of the Square Kilometre Array (SKA) and its pathfinders and precursors (Bourke et al. 2014; Staveley-Smith and Oosterloo 2015).

However, observations of the H I line in absorption due to gas in front of a bright radio continuum source have also proven to be very powerful because they allow to investigate processes and conditions in the ISM on very different spatial scales and in objects at much higher redshift compared to what is possible with emission line studies.

There are two settings for H I absorption line studies. One is intervening absorption line work where one observes gas in a foreground Galactic or extragalactic object along the line-of-sight to a distant, unrelated continuum source. Such observations are used, for example, to study the detailed properties of the ISM in our Galaxy as well as in distant galaxies, well beyond the reach of emission line observations (Kanekar and Briggs 2004).

The other setting is to observe H I where the absorbing gas is located in the same extragalactic object as where the background radio continuum is produced (usually an

AGN) and where there is an active relation between the gas and the continuum source. This is known as associated absorption work and is the topic of this review. The ISM of a galaxy with an AGN is complex with a large variety of physical conditions tracing a similarly large variety of processes. For all these situations, H I is a powerful tracer on all scales, from the pc-scales close to the central black hole to scales of many tens of kpc tracing interactions and mergers of galaxies.

Because the absorbing gas and the bright continuum source are located in the same galaxy, associated absorption studies are generally focussing on AGN and their interplay with the ISM of the same object. One of the main topics of study is the general structure and kinematics of the ISM of galaxies harbouring an AGN and how this varies among the different types of AGN. In the literature, AGN are often associated with galaxy interactions and mergers, but the real connection, if present, is still unclear. The statistics of the shapes and widths of H I absorption lines gives information on whether the ISM is likely to be in a regularly rotating structure or whether there are indications for more irregular gas distributions and thus indirectly on the role of galaxy interactions. Moreover, such studies also give information on to what extent different kinds of large- and small-scale gas structures are found in different types of AGN which, in turn, tells something about the evolution of the different types of objects. The main results from recent work on these issues are discussed in Sect. 4.

Another main topic, and which has seen major developments in recent years, is the detection of fast AGN-driven outflows of cold gas, detected as broad, blue-shifted wings in the H I absorption profiles. Such outflows are a manifestation of AGN feedback which is an important ingredient in current models for galaxy evolution and of the evolution of their central super massive black hole. H I observations of such outflows provide very useful diagnostics on how the energy released by an AGN interacts with the ISM which can be used to help to understand the physics of these interactions. These H I outflows are discussed in Sect. 5.

The third main topic we discuss is what H I absorption observations tell us about the gaseous circumnuclear regions around the super massive black hole (SMBH). Important questions are to what extent such gas can represent the fuel reservoir for the SMBH and whether it can make the difference between an SMBH being active or quiescent. It has often been postulated that H I profiles that are redshifted with respect to the systemic velocity could be signs of this feeding process, but from an observational point of view, the situation is still not clear (see Sect. 6).

Before summarising the main results obtained from observations of associated H I absorption, we highlight the observational differences between H I emission and absorption studies, we discuss how the intrinsic properties of the absorbing H I column can be derived from observations, and discuss some other technical aspects.

2 Technical aspects

2.1 Observing H I in emission and absorption: some differences

Although for emission and for absorption studies one uses exactly the same type of observations (and indeed for nearby galaxies, emission and absorption can be detected

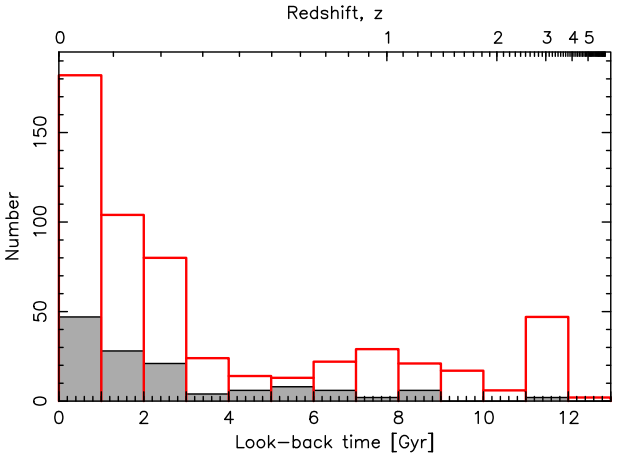

Fig. 1 The distribution of the current state of detections of associated HI absorption (shaded histogram) and non-detections (unshaded) as function of look-back time for a standard ΛCDM cosmology with $H_\circ$ = 71 km s^{-1} Mpc^{-1}, $\Omega_{\rm matter} = 0.27$ and $\Omega_\Lambda = 0.73$. Images reproduced with permission from Curran and Duchesne (2018), copyright by the authors

in the same object, see e.g. Fig. 4), compared to emission line work, HI absorption studies have both advantages and disadvantages. HI emission line observations are column density limited and because column density sensitivity scales as σ/θ^2 (with σ the noise level of the data and θ the spatial resolution), this means that, given a noise level, extended HI gas can only be detected with spatial resolutions larger than a certain limit. With the sensitivity of present-day radio interferometers, in practise this means that HI observations can trace gas structures with column densities down to a few times 10^{18} cm^{-2} at spatial resolutions of about 1 arcminute (corresponding to 60 kpc for an object at $z = 0.05$) to just below 10^{21} cm^{-2} at a few arcseconds resolution (corresponding to a few kiloparsec at the same redshift). For a given spatial resolution, sources beyond a given distance will not be spatially resolved anymore and because of beam dilution, the effective column density detection limit will increase with increasing distance. Given that the typical column densities of HI are mostly in the range 10^{19}–10^{21} cm^{-2}, this means that, unless very long observing times are used, HI emission line studies with current telescopes are in general limited to the relatively local Universe ($z < 0.1$; for exceptions see, e.g. Verheijen et al. 2007; Fernández 2016).

This is different for HI absorption observations. Because the depth in Jy of an HI absorption line depends on the strength of the background continuum source, the detectability of an HI absorption line is, everything else being equal, independent of redshift. As long as bright continuum sources exist at high redshift, HI absorption can in principle be detected as easily at high redshift as in the local Universe. Therefore, HI absorption observations are much better suited to address the evolution of the HI properties of galaxies and associated issues than emission line studies. However, in practice, relatively few detections have been made at higher redshift so far, as is shown in Fig. 1 which gives the distribution of detections and non-detections as function of

lookback time (taken from the compilation given by Curran and Duchesne 2018). This may be due to different source properties at higher redshift (either intrinsic or due to selection effects), but technical limitations of current radio telescopes (frequency coverage, sensitivity) also play a role. The fact that large ranges in redshift are not accessible due to RFI is another reason why most sources detected are at lower redshift. The highest redshift detection of H I absorption currently is $z = 3.4$ (towards TXS 0902 + 343, corresponding to a look-back time of 11.6 Gyr; Uson et al. 1991). The GMRT is currently the main instrument for high-redshift absorption line work, but with the improved low-frequency capabilities of the radio telescopes which are becoming available, (MeerKat, ASKAP, LOFAR, MWA and SKA1), the observational possibilities will much improve (see Sect. 9).

A related advantage is that H I absorption can be detected and studied at very high spatial resolutions. The column density detection limit for absorption line work is inversely proportional to the surface brightness of the background continuum. Therefore, as long as the background source remains bright enough, H I absorption can be imaged at very high spatial resolution, including the milli-arcsecond scales reached by very long baseline interferometry (VLBI). Such spatial resolutions are not accessible for H I emission, and will not be so even with the upcoming facilities. The spatial scales that can be observed with H I absorption observations can be as small as a few tens of parsecs, even in high-redshift sources. Such resolutions match very well the scales of many processes occurring in and around AGN and H I absorption observations are therefore a particularly good way to probe them. As we will see later in this review, at the much higher spatial resolutions of VLBI, H I absorption observation trace gas with similar column densities are usually detected in emission at much lower resolution.

As every observing technique, also H I absorption is affected by a number of limitations. Perhaps the main limitation is that one, and sometimes two, important parameters are ill constrained, namely the excitation temperature of the 21 cm transition (commonly referred to as the spin temperature T_s) and, in the case the continuum source is unresolved, the fraction of the background continuum that is covered by absorbing gas (the covering factor c_f). This implies uncertainties in the derived H I column densities and masses. Given the importance of this issue, we discuss this in more detail in Sects. 2.2 and 2.3.

Moreover, intrinsic to the technique is that for the gas to be observed in absorption, it has to be located in front of the radio continuum source and gas behind it will not be seen. This is obviously a limitation because we can only obtain information on the gas distribution and kinematics over the extent covered by the continuum emission (which can be quite limited). Often this is a much smaller area than the full extent of the gas structures. In addition, if H I absorption is detected, the absorbing medium can be a combination of a number of different gas clouds along the line of sight being located at different distances from the active nucleus, and one needs additional arguments, such as the width of the observed profile combined with the morphology of the background continuum, to disentangle the structure and locations of the absorbing clouds. A positive aspect of this is that absorption allows to unambiguously disentangle the kinematics of the gas in terms of whether the gas is infalling or outflowing, something often not possible with emission line observations. As we will illustrate below, this property has led to a number of very relevant results.

2.2 Basic theory of H I absorption

The study of atomic hydrogen at radio frequencies is possible thanks to the fact that a hyperfine transition exists for hydrogen atoms in the ground state ($1^2S_{\frac{1}{2}}$). Depending on the relative spins of the proton and the electron, there is a very small difference in the energy of the ground state, with the state with parallel spins having a slightly higher energy than the anti-parallel state. The energy difference between these two states is very small (5.87 μeV) so a photon associated with this transition has a frequency in the radio domain 1420.405752 MHz (corresponding to 21.106 cm). The prediction that this should be an observable transition was made by van de Hulst in 1944 when he was investigating whether there were observable spectral lines in the radio domain, and the detectability of the line was soon after confirmed in 1951 by observations done by Ewen and Purcell (1951), by Muller and Oort (1951), and by Christiansen and Hindman (1952). The theory of the 21 cm line can be found in any textbook on the physics of interstellar medium (e.g. Spitzer 1978; Field 1959; Verschuur and Kellermann 1988; Wilson et al. 2013) and here we only summarise the essentials.

The relative populations of the two energy levels of the transition can be written as $n_u/n_l = g_u/g_l \exp(-h\nu/kT_s)$ where n_u and n_l are the number of atoms in the upper and lower level, respectively and g_u and g_l the statistical weights of the two levels. T_s is the spin temperature, the commonly used term for the excitation temperature of the transition. The statistical weights are $g_u = 3$ and $g_l = 1$ and because in general $h\nu \ll T_s$, the relative populations are $n_u/n_l \simeq 3$.

Several processes, both radiative and collisional, play a role in determining the T_s of an interstellar cloud, depending on density, temperature and radiation field. We refer the reader to Field (1959) for the classic discussion of the details of this, but we will mention a few relevant aspects in Sect. 2.3.

From standard theory of radiative transfer one can easily derive that the observed spectrum $T_b(v)$ of an H I cloud with optical depth $\tau(v)$ and spin temperature T_s, and which is partially covering (with covering factor c_f) a background continuum source with brightness temperature T_c, is the combination of absorbed emission from the continuum source, the emission from the part of the continuum source not covered by the cloud, and self-absorbed 21 cm line emission from the H I cloud itself:

$$T_b(v) = c_f T_c e^{-\tau(v)} + (1 - c_f)T_c + T_s(1 - e^{-\tau(v)}).$$

The brightness T_c can be found from the line-free parts of the spectrum so that one can obtain

$$\Delta T(v) = T_b(v) - T_c = (T_s - c_f T_c)(1 - e^{-\tau(v)}). \quad (1)$$

Equation 1 shows that the spectral line will be seen either in emission or absorption depending on whether $T_s > c_f T_c$ or not. In emission line studies, it is usually assumed that the optical depth is low so that for the case of pure line emission ($T_c = 0$)

$$T_b(v) = \tau(v)T_s.$$

The observed profile $T_b(\nu)$ as function of frequency ν can be converted to a spectrum $T_b(V)$ as function of velocity V using $V = c \cdot (\nu_\circ - \nu)/\nu$ where $\nu_\circ$ is the rest frequency of the 21 cm transition. From atomic physics we know that $\tau \propto N_{\rm H\,I}/T_s$, therefore, we can obtain the H I column density from an emission line by integrating the observed emission over velocity V:

$$N_{\rm H\,I} = 1.82 \times 10^{18} \int T_b(V)[{\rm K}]\ {\rm d}V[{\rm km\ s^{-1}}], \tag{2}$$

which is independent of T_s.

If $T_s < c_f T_c$, the absorption dominates over the emission of the 21 cm line and an absorption line will be detected. Except for lower resolution absorption observations of objects in the relatively nearby Universe, for most H I absorption observations, and certainly those done with VLBI, confusion of the absorption spectrum with emission is not an issue. In other words: $T_s \ll c_f T_c$ and the observed absorption spectrum is $\Delta T(V) = -c_f T_c(1 - e^{-\tau(V)})$ and the optical depth of the H I cloud can be derived from the spectrum using

$$\tau(V) = -\ln\left(1 + \frac{\Delta T(V)}{c_f T_c}\right) \tag{3}$$

or, if the optical depth is low ($\tau \ll 1$ i.e. $|\Delta T(V)| \ll c_f T_c$)

$$\tau(V) = \frac{|\Delta T(V)|}{c_f T_c}. \tag{4}$$

The H I column density can then be found from

$$N_{\rm H\,I} = 1.82 \times 10^{18}\ T_s[{\rm K}] \int \tau(V)\ {\rm d}V[{\rm km\ s^{-1}}] \tag{5}$$

which, for faint lines ($\tau \ll 1$) reduces to

$$N_{\rm H\,I} = 1.82 \times 10^{18}\ \frac{T_s}{c_f T_c} \int |\Delta T(V|\ {\rm d}V \tag{6}$$

where all temperatures are in K and v is in km s^{-1}.

The above equation shows an important difference with emission line work namely that the column density derived from an absorption spectrum does depend on the spin temperature T_s. The reason for the difference is that in the case of optically thin 21 cm emission line, the emission is due to spontaneous transitions. Because $n_u/n_l \simeq 3$, basically independent of T_s, one can directly translate the number of detected photons into number of atoms present. The strength of an absorption line, however, depends on the detailed balance between absorbing and emitting photons along the line of sight and this does depend on T_s.

In addition, the derived column densities also depend on the covering factor c_f which often is unknown. This dependence of $N_{\rm H\,I}$ on T_s and on c_f is a significant

complication for many absorption line studies. We will briefly discuss this in the following section.

2.3 Spin temperature and covering factor

The discussion of the previous section shows that there are two main parameters that introduce uncertainties in the estimate of the HI column density derived from absorption observations: the spin temperature T_s and the covering factor c_f.

The spin temperature T_s is often the one more difficult to constrain. A number of factors control the spin temperature of atomic hydrogen (see, e.g. Field 1959): absorption of photons from the radiation field, emission stimulated by such photons, collisions of H atoms with other particles, and pumping by Lyα photons. In the normal ISM of a galaxy, collisions dominate the excitation of the line. Radiative effects are particularly important in the vicinity of an AGN and can give rise to high spin temperatures, depending on gas density. Under such conditions the spin temperature can be as large as a few thousand K, up to 8000 K (Bahcall and Ekers 1969; Maloney et al. 1996) and there is observational evidence that this indeed occurs.

The HI in the normal ISM of a normal galaxy is formed by a mix of phases, each with different densities and temperatures. Such ISM is typically divided in a colder, denser phase (the cold neutral medium; CNM) and a warmer, less dense phase (the warm neutral medium; WNM). The typical temperatures of the CNM are around 100 K while those of the WNM are in the range 1000–7000 K. In the normal ISM of galaxies, the spin temperature approaches the kinetic temperature because the transition is collisionally excited. The existence of two phases of HI in the typical ISM means that there are also two regimes for T_s.

However, since $\tau \propto T_s^{-1}$, HI absorption observations are more sensitive to the colder components of the gas and the effective T_s of an absorption line due to a number of intervening clouds with a different value for T_s is the harmonic mean of the T_s of all intervening clouds. In many HI absorption studies a canonical $T_s = 100$ K is assumed, but there are many situations where a higher T_s is more appropriate. For example, for HI clouds in the Milky Way, a relation between T_s and N_{HI} has been observed in the sense that a threshold exists (around $N_{HI} \simeq 2 \times 10^{20}$ cm^{-2}) below which the T_s of absorbing clouds is high (800–7000 K) while for clouds with N_{HI} above this threshold, T_s is only a few hundred K (Kanekar et al. 2011). This threshold is thought to arise because inefficient self-shielding against ultraviolet photons at lower column densities prevents the formation of the CNM.

Low spin temperatures have been found in some radio sources. One case is Centaurus A where HI absorption is detected against the Northern and beginning of the Southern lobe, i.e. absorption on scales of a few hundred parsec to one kiloparsec and not in the vicinity of the central AGN. By comparing the strength of the absorption with that of emission from neighbouring positions, a spin temperature of $T_s \sim 100$ K was found (Struve et al. 2010b). However, this absorption occurs quite far from the central AGN and may not be not representative for absorption by clouds closer to the AGN.

An example of higher T_s is the young radio source PKS 1549-79 (Holt et al. 2006) for which an independent estimate of the neutral column towards this source was made based on the optical extinction derived from modelling the optical continuum of the quasar. By comparing this estimate with the HI absorption data, it was found that the spin temperature must be in the range $3000 < T_s < 6000$ K. However, given its properties, this object could be an extreme example. Other methods for putting limits to the T_s, e.g. using X-ray observations, have given less extreme values, see Sect. 8.

The covering factor c_f is often assumed to be unity, mostly due to lack of information that can be used to motivate another value. Curran et al. (2013a) pointed out that apparent systematic differences could exist between the covering factor of compact and of extended sources, simply for geometrical reasons due to differences in size between the two classes of sources, even if there is no difference in the intrinsic properties of the absorbing gas in the two types of sources. However, VLBI observations suggest that their model may be too simple (see Fig. 2). For example, the covering factor is close to $c_f = 1$ in the compact source PKS 1946+708 (Peck et al. 1999), but examples of compact sources with much lower covering factor also exist (e.g. $c_f \sim 0.2$ in B2352 + 495, Araya et al. 2010, or in 4C 12.50, Morganti et al. 2013). Extended sources with a large covering factor are also known (e.g. $c_f = 1$ in the re-started source 3C 293 Beswick et al. 2004). However, a covering factor of a few percent is measured in the extended source NGC 315 (Morganti et al. 2009a), while $c_f = 0.5$ is found for the extended source 3C 305 (Morganti et al. 2005b). These examples suggest that size is not always a good predictor for the covering factor (see also Sect. 4.2.3)

2.4 Current and future telescopes and their limitations

HI absorption observations have been carried out with all available radio telescopes. First observations were done using single dish telescopes [(such as Arecibo, Parkes, and the Green Bank Telescope (GBT)], but most of the recent work has been done with interferometers: VLA, ATCA, WSRT, GMRT and very long baseline interferometry network [mainly European VLBI Network (EVN) and very long baseline array (VLBA)]. Interferometers provide high spatial resolution which is a distinct advantage, given that associated absorption is typically found in the very central regions of galaxies. They also have better spectral stability of the observing band and are less affected by RFI. The recent upgrades of many radio telescopes have further improved the capabilities and performance for HI absorption observations.

A number of limitations have affected HI absorption observations in the past. One is the limited velocity range that could be covered by an observation while maintaining good spectral resolution. This was due to the relatively small width of the observing bands available at the time combined with limited correlator capacity. In many objects, the width of the absorption profile exceeds 1000 km s^{-1} which in the past was similar, or even larger, than the velocity range covered by the observations. Due to upgrades, all relevant radio telescopes now allow observations with very large bandwidth with good velocity resolution and this has resolved this issue. Parallel with this development has been the improved spectral stability of the instruments through the use of digital systems. While 15–20 years ago it was difficult to obtain a spectral dynamic

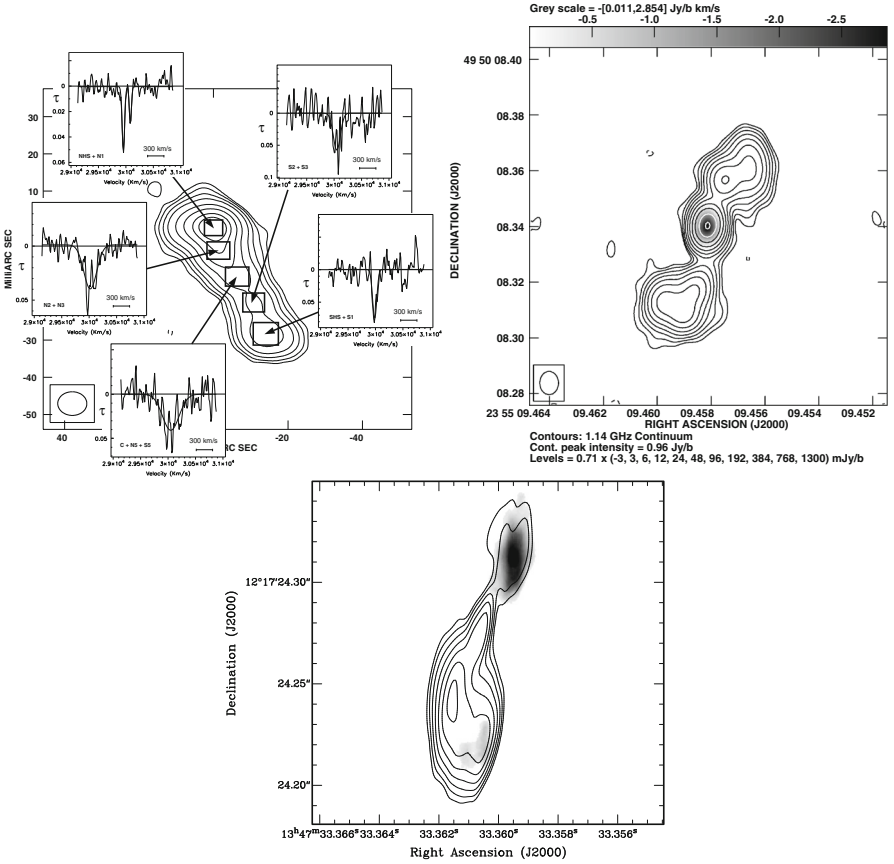

Fig. 2 Three examples showing extreme cases for the covering factor. For PKS 1946 + 708 shown in the top-left panel, absorption is detected across the entire source and thus $c_f = 1$. In the source in the top-right panel (B2352 + 495), absorption is only detected against the core, resulting in a low covering factor of $c_f \sim 0.2$, while the bottom panel shows the opposite situation with a similar covering factor, but where absorption is only detected against part of the radio lobes (4C12.50; data taken from Morganti et al. 2013). Images [top] reproduced with permission from Peck et al. (1999) and Araya et al. (2010), copyright AAS

range better than 1:1000, current instruments perform at least a factor 10 better. This means that, in particular, broad but faint absorption components can now be detected much more easily. The combination of broader observing bands and better spectral dynamic range has provided a major step forward and new discoveries have resulted (see Sect. 5.1).

Another main limitation has been, and to some extent still is, the limited coverage and sensitivity at lower frequencies which makes it harder to study high-redshift objects. Only a few radio telescopes are fitted with receivers suitable for observing HI at redshifts higher than 0.2–0.4 and the few receivers that were available in the past, for example, the UHF receivers mounted on the WSRT until a few years ago, had relatively high system noise. The situation has improved with the recent upgrade of the GMRT which offers continuous frequency coverage with good sensitivity, bandwidth

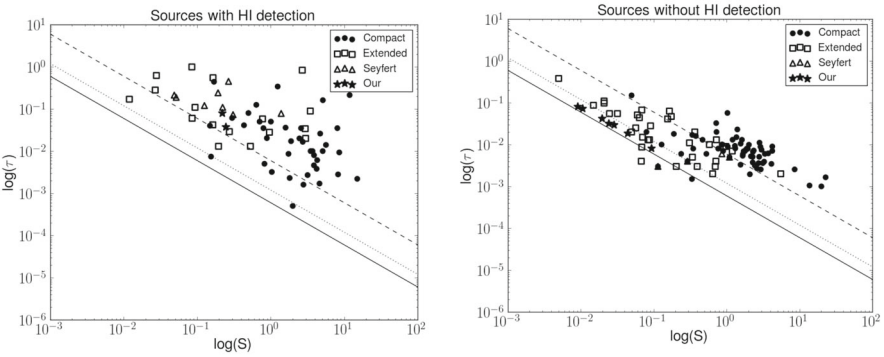

Fig. 3 Optical depth vs flux density for H I detections (top) and non-detections (bottom) collected from the literature. The solid, dotted and hashed line represent the 3σ limits in the absorption line signal corresponding to $1\sigma = 0.2, 0.4, 2$ mJy. Image reproduced with permission from Geréb (2014), copyright by the author

and spectral resolution up to high redshifts (Gupta et al. 2017). An important problem is, of course, that many frequency ranges below 1300 MHz are very significantly affected by RFI so that many redshift ranges are not observable. The possibilities for high-z observations will improve with advent of MeerKat, which is located at a relatively RFI-poor site in South Africa and which will have very good sensitivity up to redshifts of 1.4, and in particular with ASKAP in Western Australia which can observe up to $z = 1$ and for which the RFI situation for redshifts higher than about 0.4 is particularly good. Ultimately SKA1-MID will allow studies up to $z \sim 3$ and with SKA1-LOW for even higher redshifts.

This new generation of radio telescopes will also offer an important improvement (a factor 10 or more) in sensitivity, even at low redshifts, which obviously is currently another limitation for H I absorption observations. To give an example, for a velocity resolution of 10–20 $\mathrm{km\,s^{-1}}$ (which is commonly used because it provides a compromise between velocity resolution and sensitivity, i.e. observing time), a telescope like the VLA can reach—for an observation of a several hours—a typical rms noise per channel of $\sim$ 0.3 mJy $\mathrm{beam^{-1}}$. This means that for a radio source of 100 mJy one can detect a peak optical depth of $\tau \sim 0.015$ (i.e. the flux absorbed by the H I is a few percent of the radio continuum of the source). This opacity level is where currently the bulk of the detections have been found, while objects with optical depth above 0.1 are rare. Figure 3, which plots the 1.4 GHz continuum flux density of sources against the peak optical depth (τ_{peak}) for detections and non-detections (taken from Geréb 2014), shows that there is no evidence for any trend of optical depth with source brightness. This means that with more sensitive observations fainter source populations will be detected in H I absorption. The figure also shows that some upper limits are very tight and deeper than the level of typical detections. This shows that there is a population of radio sources that does not contain H I, which can be valuable information about the nature of these sources. However, many upper limits are at the same level as most of the detections, thus they are not very constraining about the absence or presence of absorption in those sources. Higher sensitivity will allow to better separate these different populations.

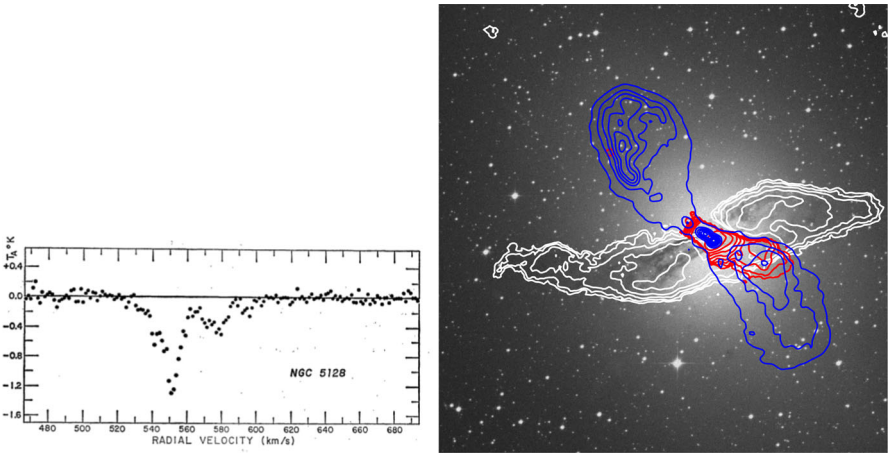

Fig. 4 Profile of the first HI absorption detection which was obtained against the central region of Centaurus A with the NRAO 140-foot telescope. On the right, we illustrate the geometry of the HI absorption using the resolved image of the same region made with the Australia Telescope Compact Array. Superposed to an optical image, the blue contours represent the radio continuum coming from the inner lobes of Centaurus A, the white contours trace the HI emission from the warped gas disk of the host galaxy, while the red contours represent the HI detected in absorption against part of the continuum emission. In this object, most of the gas observed in absorption is that part of the large-scale disk that happens to pass in front of the radio continuum. This allows to constrain the geometry of this disk relative to the continuum lobes. Image (left) reproduced with permission from Roberts (1970), copyright by AAS; (right) adapted from Struve et al. (2010b)

3 AGN seen through H I absorption: an overview

Over the years, HI absorption studies have given important new insights into the structure of the gaseous medium in the vicinity of an AGN, into the distribution and kinematics of gas in the nuclear regions of active galaxies, into the role gas may play in the evolution of AGN, and vice versa into the influence AGN can have on the gas properties of galaxies. In the following sections we present this in detail, but here we briefly summarise the main results and put them in the context of earlier work.

One important aspect of the early studies has been that they established the presence of HI even in the circumnuclear regions of AGN, and that they demonstrated the feasibility and the potential of HI absorption studies for better understanding many AGN-related phenomena. The first detections of HI absorption were made against the central region of the iconic radio galaxy Centaurus A by Roberts (1970, see Fig. 4) and in the nearby spiral galaxy NGC 4945 (Whiteoak and Gardner 1976). This was followed by the detection of HI absorption in another famous radio galaxy, 3C 84 (Perseus A), where—similar to what is seen in optical emission lines—two absorption systems were found at very different velocities by De Young et al. (1973) and Crane et al. (1982); see also Sect. 4.3.

Since then, the earlier studies of associated HI absorption in extragalactic sources were mostly motivated by tracing the presence of nuclear disks and the presence of infalling gas fuelling the AGN. Indeed, the first HI observations of radio-loud galaxies (e.g. Dickey 1982; Mirabel 1982; Shostak et al. 1983; Heckman et al. 1983) have shown

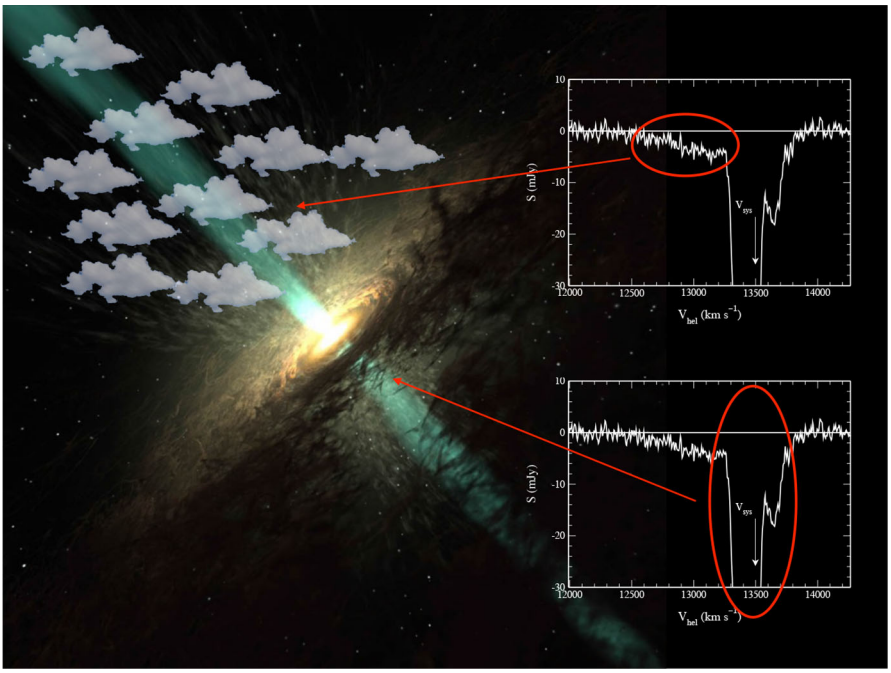

Fig. 5 Illustration of common structures of absorbers and the related H I profiles. Deep absorption profiles with widths of up to a few hundred km s^{-1} centred on the systemic velocity of the galaxy originate from regularly rotating gas disks which are projected on the bright inner radio continuum emission. Asymmetric wings to the absorption profile are in general associated with unsettled gas structures, such as gas outflows driven by the radio jet, or tidal gas streams

that the H I was likely associated with disk structures with column densities about a factor 10 higher than of the H I in the Milky Way and having a thickness of 10^2–10^3 pc which was derived from a trend between column density and inclination of the disk derived from optical images (Heckman et al. 1983). Typically, these spectra have deep absorption with a full-width half maximum (FWHM) up to a few hundred km s^{-1}, symmetric with respect to the systemic velocity of the host galaxy. This suggests the H I gas is tracing a regular rotating structure (see the bottom panel in Fig. 5 for an example). The conclusions of these initial studies were mostly focused on showing the widespread presence of gas disks relevant for understanding the structure of the central regions and for unified schemes for AGN. Many current studies still focus on the large-scale properties of the absorbing gas structures, whether they are regular or not, and their relation to the evolution of the AGN and of the galaxy that hosts the AGN. The group of recently born, young radio sources, i.e. compact steep spectrum (CSS) and gigahertz peaked spectrum (GPS) sources (as well as restarted radio sources) are those having the highest H I detection rate and they will appear prominent in this review (see more in Sect. 4.2.3). Interesting is that recent studies have uncovered more examples of circumnuclear disks and tori on scales smaller than a kpc (i.e. tens to a few hundred pc). Such gas close to the BH is typically characterised by broader absorption

profiles with widths of several hundred $\mathrm{km\,s^{-1}}$ (e.g. Cygnus A, Conway and Blanco 1995; Struve et al. 2010b; Peck and Taylor 2001, see more in Sect. 4.2.2).

Following the initial studies, van Gorkom et al. (1989) expanded the samples and found evidence that HI absorption lines redshifted relative to the systemic velocity occur relatively more often than blueshifted absorption lines. This suggests that the HI could be involved in the fuelling of the AGN. For quite a period, largely based on this work, the perception in the community has been that redshifted absorption occurs quite often. However, separating infalling gas from the one regularly rotating has proven to be more challenging than expected because of the similar amplitudes of both infalling and rotational velocities, as also shown by some of the more detailed studies (e.g. O'Dea et al. 1994; Taylor et al. 1999; Maccagni et al. 2014; Tremblay et al. 2016, see also Sect. 6).

Subsequent larger surveys have indeed confirmed that the situation is more complex and, in particular, in the last 15 years, several studies have shown that the situation may actually be the reverse, namely that blueshifted absorption occurs relatively more often (Vermeulen et al. 2003a). In fact, after the first discovery (Morganti et al. 1998, 2003), many examples are now known of very broad, shallow ($\tau \ll 0.01$) blueshifted absorption components which indicate fast HI outflows driven by the AGN or by a cocoon inflated by the AGN (see Sect. 5.1). In some cases these outflows are located off-nucleus (so far they have been found up to a few hundred pc from the nucleus) at the location of bright radio components. Together with the high occurrence of outflows in newly born (or reborn) sources (see Sect. 4.2.3), this suggests that, at least in some objects, the radio jets can play a role in driving them. This discovery has changed many ideas about the relation between an AGN and the gas in its immediate vicinity. The possible relevance of these outflows in connection with the role of AGN feedback in the context of galaxy evolution was recognised immediately. The discovery of HI outflows can have a similar outflowing component of molecular gas (Feruglio et al. 2010) has further confirmed the relevance of the cold AGN outflows.

4 The nature of the absorbing structures in the various types of radio sources

For a large fraction of the detections, the HI absorption in radio sources is seen against their central regions. Because of this, it allows to probe the physical conditions of the gas in the inner regions of radio sources and the nuclear structure of the various types of AGN. The "zoo" of AGN is very rich (see Padovani 2016 for a review) and as described in several papers (see, e.g. Heckman and Best 2014; Ramos Almeida and Ricci 2017 for recent reviews), the nuclear regions of AGN of different (radio) luminosity are expected to show differences in the distribution and physical conditions of the gas and dust.

In particular, two main types of AGN have been identified and, following Heckman and Best 2014, referred to as radiative-mode and jet-mode AGN. Early studies proposed (e.g. Krolik 1988) for the first group, where the energy released is dominated by radiation, that the SMBH is surrounded by an accretion disk and, on larger scale, an obscuring structure, usually referred to as *torus*, is present. The physical state of the

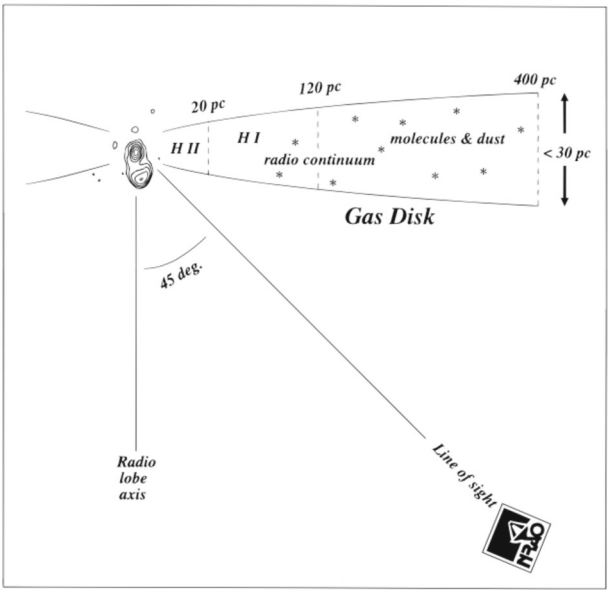

Fig. 6 A sketch of the conditions of the gas in the circumnuclear disk of Mrk 231, illustrating the general models for the structure of circumnuclear disks of, e.g. Maloney et al. (1996). The inner part of the gas disk is ionised while the outer regions consist of cooler molecular gas and dust. In between is a warm transition zone containing atomic hydrogen. Image reproduced with permission from Carilli et al. (1998a), copyright by AAS

gas near an active nucleus has been described by, for example, Maloney et al. (1996). The torus will be molecular if its pressure exceeds a critical value which depends on the luminosity of the central source, the distance from the source, and the attenuating column density between the central source and the point of interest in the torus. Under certain conditions, the torus can also have a significant component of atomic hydrogen. If the pressure is below this critical value, the gas is warm ($T \sim 10^4$ K) and atomic(Maloney et al. 1996).

These models predict that at the inner edge of the disk, likely between 0.3 and 1 pc from the AGN, a region of depth $\sim$ 0.1 pc is fully ionised at a temperature of $\sim 10^4$ K and with a density of a few $\times 10^4$ cm^{-3}. Such ionised gas will radiate thermal emission and will cause free–free absorption of nuclear radio components viewed through the torus. Going outward, a warm transition zone is present, traced by H_2O maser emission and by HI absorption. Further outward, a cooler molecular zone exists. The conditions of the gas also change with the vertical distance from the mid-plane of the disk/torus. The most recent theories suggest that the tori/disks are likely to be clumpy and that they even can be warped (e.g. Ramos Almeida and Ricci 2017), features which could be detectable using the high spatial resolution provided by VLBI observations. A sketch of a model of this kind, as applied to the structure of the inner disk/torus of Mrk 231, is given in Fig. 6.

On the other hand, jet-mode AGN are instead associated with low accretion-rate and radiatively inefficient processes. Thus, an accretion disk and/or torus are likely

absent, but the reservoir of gas can be in the form of larger circumnuclear disks (on scales of tens to hundred of pc).

Apart from their role in determining the differences between the physical properties of the AGN, these inner gas structures are also relevant for how we see and classify AGN, depending on to what extent they obscure our view of the AGN and its immediate surroundings (as in the unified schemes). In addition, they are also thought to play a key role in feeding the SMBH. Because of all this, a large effort has been dedicated also to trace the presence of H I in these structures.

In the case of radio AGN, powerful radio galaxies (i.e. the so-called Fanaroff–Riley type II, FR-II, radio galaxies) and low-power, edge-darkened radio galaxies (Fanaroff–Riley type I, FR-I, radio galaxies) follow, to first order, the separation between radiative-mode and jet-mode AGN (but see Heckman and Best 2014 and Tadhunter 2016 for more details and exceptions).

Signatures of the presence of tori in FR-II has been found by observations in various wavebands (see Tadhunter 2016). However, the search for H I in these structure has given mixed results, as described below.

On the other hand, in low-power, edge-darkened radio galaxies (Fanaroff–Riley type I, FR-I, radio galaxies), the observations support the absence of a thick torus and indicate that the gas and dust is distributed in larger, thinner circumnuclear disks. For example, unresolved optical cores (e.g. seen in HST images, Chiaberge et al. 1999) are commonly present in FR-I radio galaxies. The flux of these optical cores appears to correlate with their radio core flux, arguing for a common non-thermal origin (i.e. synchrotron emission from the relativistic jet) and supporting the absence of a pc-scale geometrically thick, obscuring torus in FR-I radio galaxies. The presence of H I in these circumnuclear structures is confirmed by the results described below.

To derive information about the kind of H I structures that are detected in absorption, it is useful to know more about the larger H I structures seen in emission, often unrelated to the AGN activity, in nearby early-type galaxies, i.e. the typical host of radio galaxies. Such early-type galaxies have historically been considered red-and-dead, but in recent years it has become clear that many early-type galaxies have significant amounts of gas, including atomic hydrogen (see Morganti et al. 2006; Oosterloo et al. 2010; Serra et al. 2012 for some statistical results on the large-scale H I emission in early-type galaxies). The best sample to use as a reference point is the ATLAS^{3D} sample (Cappellari et al. 2011) for which a broad suite of multi-wavelength observations are available, including deep imaging of the H I emission (Serra et al. 2012). This sample consists of nearby early-type galaxies, most of them without a strong (radio) AGN (Nyland et al. 2017). Based on H I observations of a large fraction of the ATLAS^{3D} galaxies, Serra et al. (2012) find that in about 40% of those residing in the field, H I emission is detected. In many cases, the H I is found to form a large-scale H I disk, but also irregular structures, like tails and filaments, were observed in many galaxies. This suggests that for non-cluster radio sources there can be components in the absorption spectra that are not related to the circumnuclear environment. In a few members of the ATLAS^{3D} galaxies H I absorption is detected and these spectra suggest that the profiles produced by these large, regular structures are typically relatively narrow (between 70 and 100 km s^{-1} FWHM) and centred on the systemic velocity of the host galaxy (Serra et al. 2012).

Only a small fraction of the absorption profiles in radio galaxies are as narrow as those found in radio-quiet galaxies (i.e. like those in ATLAS^{3D}) and these narrow lines are mostly found at low radio power (Maccagni et al. 2017). In most other cases, the absorption is typically several hundred $\mathrm{km\,s^{-1}}$ wide. This suggests that in addition to possible absorption from large-scale disks, radio galaxies also have H I distributed in other components, for example, much closer to the central radio source. If a rotating disk is closer to the centre, a larger range of velocities project on a background continuum source of a given size and hence produces a larger profile width.

Below we go in more detail in describing the relevant results on central gas structures obtained for different groups of AGN. Seyfert galaxies and radio galaxies are presented separately because they typically (albeit with some exceptions) are hosted by different type of galaxies: Seyferts in spiral galaxies (where large-scale gas disks are expected to be present) and radio galaxies in earlier-type galaxies.

4.1 H I absorption in nearby galaxies and Seyfert galaxies

For nearby galaxies, the study of H I in absorption has been focussed on Seyfert galaxies and on interacting, FIR-bright and some peculiar galaxies.

Early studies of H I in the nuclear regions of Seyfert galaxies were carried out by Dickey (1982) while the most complete study up to now has been done by Gallimore et al. (1999). In the latter work, 13 galaxies were observed which were selected as a flux-limited sample of spiral galaxies with evidence for nuclear activity and having a radio brightness $S > 50$ mJy. These observations show a high detection rate, with 9 detected objects having a column density ranging between 5×10^{20} and 10^{22} $\mathrm{cm^{-2}}$ assuming $T_s = 100$ K. Furthermore, there is a weak correlation between the probability to find H I absorption and the inclination of the host galaxy and similarly for the observed H I column density. Figure 7 shows the H I absorption from one of the galaxies, NGC 2992.

A main result of Gallimore et al. (1999) is that no H I absorption is detected against the central, pc-scale, radio sources, even in known obscured Seyfert galaxies like Mrk 3 or NGC 1068. In general, the absorption is detected against extended radio jet structures and appears to avoid central compact radio components. Extensive modelling by Gallimore et al. (1999) suggests that the H I absorption appears to trace rotating gas disks on the 100 pc-scale, which are aligned with the outer, larger disks of the host galaxy, rather than gas associated with the very central (pc) regions of the AGN. The trend between the H I column density and the inclination of the disk (see Fig. 7, right) is consistent with this. Among the possible explanations for the result of Gallimore et al. (1999) is that free–free absorption suppresses the central background source so that H I absorption cannot be detected against it.

Another example of this is seen in high-resolution observations of the nearest quasar, Mrk 231, studied in detail by Carilli et al. (1998a) using both VLA and VLBA. They found a rotating disk with an east–west velocity gradient of about 110 $\mathrm{km\,s^{-1}}$ traced by H I absorption against a diffuse component on scales of hundred parsecs. However, this absorption disappears when full resolution spectra are taken only from the core. Thus, also in this object the absorption is not against the pc-scale radio core, but against a

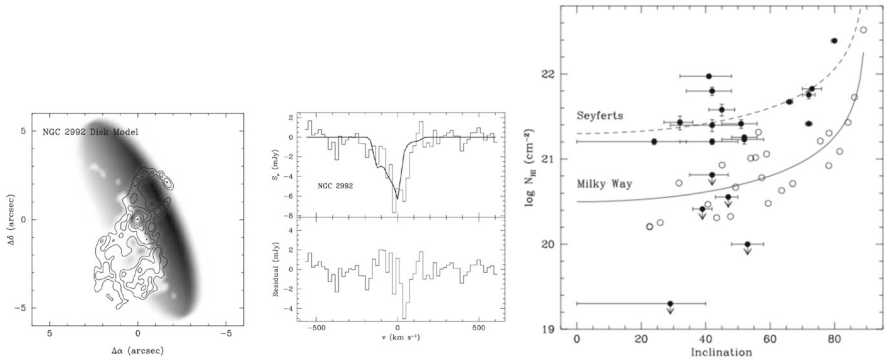

Fig. 7 Left: The H I absorption in NGC 2992 and the model of the absorbing structure and orientation respect to the continuum. Right: Distribution of column density for various groups of sources. The columns density derived for the Seyfert galaxies assume a characteristic T_S= 100 K. Images reproduced with permission from Gallimore et al. (1999), copyright by AAS

more diffuse radio continuum component seen on hundred pc scales. A circumnuclear disk similar to those used by Gallimore et al. (1999) in their modelling can be invoked to explain these findings, where in this case the H I is located at a few tens of parsec from the BH. The only Seyfert galaxy where, so far, H I absorption associated with a small (pc-scale) disk/torus is NGC 4151 as reported by Mundell et al. (1995).

However, the presence of at least some H I gas located close to the AGN cannot be excluded by observations at high (tens of mas) spatial resolution. This is the case, in particular, in Seyfert galaxies that show evidence of a particular rich and dense nuclear ISM by the presence of water masers as, for example, in NGC 5793 (Pihlström et al. 2000) and TXS 2226-184 (Taylor et al. 2002, 2004). Eight galaxies have been reported to exhibit both water masers and H I absorption (Taylor et al. 2002). There appears to be a fair amount of overlap between the presence of water megamasers and H I absorption, although the search in five sources with H I optical depth larger than 0.1 did not bring new detections. Whether this is due to the structure of the central disk/torus or on the conditions of the medium is still unclear (Taylor et al. 2002).

The column densities of the H I absorption is often compared with the column densities derived from X-ray observations. This will be discussed in more detail in Sect. 8. In the case of Seyfert galaxies, Gallimore et al. (1999) did not find a correlation between the column densities derived in these two ways, with those estimated from the X-ray absorption systematically higher. The mean column density from H I absorption is $\sim 10^{21}$ cm^{-2} (with cases up to 10^{22} cm^{-2}) assuming $T_s = 100$ K, while it is $\sim 10^{22.5}$ cm^{-2} for the mean hydrogen column density derived from soft X-ray observations. This is possibly indicating that the radio and the X-ray sources are not co-spatial (see Sect. 8).

No evidence for substantial infall/outflow of neutral hydrogen was found by Gallimore et al. (1999) and they concluded that in the Seyfert galaxies they studied, the atomic gas is mainly in rotating structures. However, this result is likely affected by the limitations of the telescopes used at the time, in particular, the limited bandwidth. Fast H I outflows are now known in a number of Seyfert galaxies and their detection

was only possible due to the broader observing bands available currently. Tentative evidence of H I outflows was already presented for two objects (NGC 1068 and the starburst/Seyfert galaxy NGC 3079) where broad ($\geq$ 600 km s^{-1}) absorption features were found by Gallimore et al. (1994). The presence of a faint blueshifted feature in the spectrum of NGC 3079 has been confirmed by more recent observations (Shafi et al. 2015). Furthermore, clear cases of broad, blueshifted wings of H I absorption indicating gas outflowing at high velocities ($\sim$ 1000 km s^{-1}) have been found in the Seyfert 2 galaxy IC 5063 and in the nearby quasar Mrk 231. IC 5063 is the clearest example of an H I outflow and one of the best studied cases of AGN-driven outflows so far (Morganti et al. 1998; Oosterloo et al. 2000) and for which now also a strong molecular counterpart has been detected (see more in Sect. 8). More about H I absorption as a powerful way to trace gas outflows will be discussed in Sect. 5.1.

H I absorption can also be used to disentangle the complex distribution of the gas in the centre of interacting systems (e.g. Mrk 1; Omar et al. 2002; Srianand et al. 2015) and in large merging systems, like Arp 220 (Mundell et al. 2001; Allison et al. 2014) and NGC 6240 (Beswick et al. 2001; Baan et al. 2007, and references therein). Such systems typically show broad H I absorption profiles that are tracing disturbed disk-like structures. The presence of broad profiles in such cases is confirmed for the major-merger systems included in the survey of radio sources selected from cross-correlating SDSS and FIRST (Geréb et al. 2015; Maccagni et al. 2017), which show absorption profiles with full widths up to 800 km s^{-1}.

A final remark is about the peculiar galaxy NGC 660 which is well-known for its prominent large, warped disk and in which in the central regions H I absorption is detected (Baan et al. 1992). Interestingly, the AGN in the galaxy has recently gone through an outburst which has produced a new, bright radio continuum structure in the core of the galaxy. The appearance of this new continuum component has affected the shape and depth of the H I absorption profile. Changes have been observed in some of the components of the profile, for example a slightly broader redshifted wing, suggesting inflow of material along our line of sight (Argo et al. 2015). Whether there are more objects where changes in the profile shape occur due to changes in the H I (on H I coverage) it is still an open question. Campaigns to investigate this are still too time consuming, but will be done as result of the deep observations in upcoming surveys.

4.2 H I absorption in radio galaxies

A fairly large number of studies have presented observations of H I absorption in radio galaxies (e.g. Morganti et al. 2001; Vermeulen et al. 2003a; Gupta et al. 2006; Curran et al. 2008; Chandola et al. 2011; Allison et al. 2012, 2014; Geréb et al. 2015; Aditya et al. 2016; Glowacki et al. 2017; Maccagni et al. 2017, for some examples) . In addition, an analysis of a compilation of all data published so far has been presented by Curran and Duchesne (2018). These studies typically show a detection rate of H I absorption around 20–30%. To first order, the detection rate appears to be independent of radio power throughout the more than 5 orders of magnitude of radio power sampled in recent surveys. This holds also for low radio powers ($P < 10^{23}$ W Hz^{-1}) where the

separation between radio galaxies and radio-quiet, normal galaxies becomes fuzzy. The similarity of the detection rate of H I absorption and H I emission suggests a continuity between what found (in emission) for radio-quiet, nearby early-type galaxies and radio galaxies. The only study were a combination of H I in emission and in absorption has been traced in a sample of radio galaxies has been done by Emonts et al. (2010). The results of this study appear to support this continuity, albeit that the statistics and the depth of the observations will need to be improved to confirm the results.

The column densities of the H I absorption in radio galaxies are typically between a few times 10^{20} and 10^{21} cm^{-2} for $T_s = 100$ K. Barring uncertainties in T_s, it appears that the typical column densities in radio galaxies are somewhat lower compared to those seen in Seyfert galaxies where column densities up to 10^{22} cm^{-2} are observed. However, some of the absorption lines may come from gas located quite close to the AGN where T_s can be much higher and, as a consequence, also the column density.

Below we discuss how these different structures can be identified thanks to statistical consideration or high-spatial resolution observations.

4.2.1 Circumnuclear disks and tori in radio galaxies

As described above, the inner gas disks of powerful radio galaxies (FR-II) and of low-power radio galaxies (FR-I) are thought to be very different in size, thickness and density. The AGN in an FR-II galaxy is surrounded by a small, thick torus while in FR-I objects the central gas and dust is distributed in a large, thinner circumnuclear disk (see Fig. 6). Based on this picture, and assuming H I is present in all these structures, the detection rate and properties of H I absorption should be different for the two classes of radio galaxies, for example, a higher detection rate would be expected in FR-II objects compared to FR-I sources. Moreover, the detection rates should also depend on the orientation of the nuclear disk. Testing the hypothesis of differences in the structure of the central region of FR-II and FR-I is, however, not entirely straightforward and the observations are affected by a number of limitations. For example, performing H I absorption observation of powerful radio galaxies is not always easy. The radio flux of their core is typically relatively low (see, e.g. Giovannini et al. 1988; Morganti et al. 1997) making difficult to reach, with standard observations, sufficient optical depth sensitivity.

Most of the evidence for circumnuclear structures comes from statistical studies which we summarise below. However, some exceptions like the one from high-resolution, down to pc-scale, VLBI observations (Sect. 4.2.2) and, e.g. the observations of the nearest radio galaxy Centaurus A allow to trace the circumnuclear structures in detail.

Given its proximity, Centaurus A represents a special case for the detection and study of a circumnuclear disk in an FR-I radio galaxy. Not only the H I absorption, but also the H I emission of this galaxy can be studied in detail. The position–velocity diagram of Fig. 8 illustrates how a circumnuclear disk can be identified from the H I observations (Morganti et al. 2008). The position–velocity plot shows how the kinematics of the large dust lane and disk (seen in emission, grey scale) cannot explain the large velocity range seen in the very centre (region in black representing the absorption). Instead, the nice correspondence of the inner, broad H I absorption with the 160

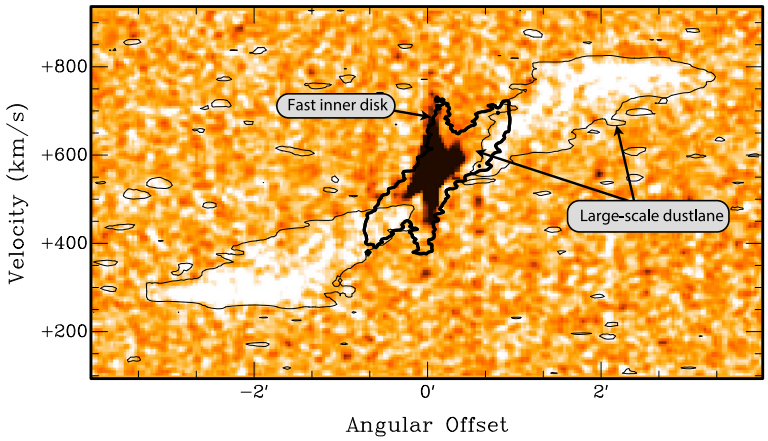

Fig. 8 Position–velocity plot of the H I (grey-scale and thin contours) in Centaurus A, taken along position angle 139°, with superimposed the CO emission (thick contours; from Liszt 2001). The grey-scale represents the high-resolution H I data (beam 8 arcsec) while the thin contour is from the same dataset smoothed to 15 arcsec. Note that the CO observations do not extend beyond a radius of about 1 arcmin. Image reproduced with permission from Morganti et al. (2008), copyright by ESO

pc sized inner H_2 disk (in emission, thick black contours) detected in Centaurus A (Liszt 2001), strongly suggests that the central H I absorption also traces this circumnuclear disk. This can be used as template for other radio AGN where such resolution cannot be reached.

The expected differences between the nuclear regions of FR-I and II have been mainly addressed by statistical studies. For example, using a flux limited sample of radio galaxies, Morganti et al. (2001) found that in powerful FR-II radio galaxies, no H I absorption was detected in the few galaxies observed that have broad (permitted) optical lines, while three out of four galaxies with narrow optical lines were detected (the one non-detection having quite a high upper limit). This is consistent with what is expected according to the unified schemes which predict that the presence of broad optical lines indicates an unobscured view of the AGN, while narrow optical lines means that the torus is blocking the view of the AGN and hence can also cause H I absorption. The same study suggested that the detection rate of H I absorption in FR-I objects is low: only one of the 10 FR-I galaxies observed was detected in H I absorption, consistent with the idea that their cores are relatively unobscured. Similar results have been obtained by Gupta and Saikia (2006), Gupta et al. (2006) and by Chandola et al. (2013). The latter study, using new observations combined with the literature data, found H I absorption towards 4 out of 32 ($\sim$ 13%) FR-I objects, and towards 3 out of the 15 ($\sim$ 20%) FR-II sources observed. However, considering the small samples of all these studies, it is difficult to make firm conclusions about differences in the torus/disc structure between FR-I and FR-II sources.

The distribution of dust in the central regions of FR-I radio galaxies has been further investigated in the study of van Bemmel et al. (2012), by combining HST images, tracing the dust, with H I absorption observations. As expected, they found that the occurrence of H I absorption is linked to the presence of dust. They also found

that the absence of HI absorption correlates (to first order) with the presence of an optical core (hence an unobscured view of the AGN), while an optical core is not detected if $N_{\rm HI} > 10^{21}$ cm^{-2} . These results are again consistent with the neutral gas and the dust being associated with the kiloparsec-scale disks and do not require parsec-scale dust tori to be present in FR-I radio galaxies.

However, it is important to keep in mind that the detection rate is also related to the more general conditions of the interstellar medium. For example, a link between presence of HI and dust has been seen using IR colours. Maccagni et al. (2017), using data from the WISE satellite, report a detection rate of almost 40% for sources bright at 12 and 4.6 μm and that are thus rich in AGN-heated dust. On the contrary, for dust-poor galaxies the detection rate is as low as 13%. From shallower observations of a sample of compact-core radio galaxies, Glowacki et al. (2017) confirm the detection rate in early IR type radio galaxies but found a lower detection rate (i.e. 6 ± 4%) in late IR type objects. The low number statistics together with the different type of radio sources and depth of the observations, make difficult to explain this difference. These statistical studies are still at the beginning and they will highly benefit from the upcoming large surveys (Sect. 9). Finally, Chandola and Saikia (2017) find significant differences in the distributions of WISE W2(4.6μm)–W3(12μm) colour between sources with HI absorption detections and the non-detections. They also report a very high detection rate of 70 ± 20% for low-excitation radio galaxies (LERGs) with W2–W3 > 2 and having compact radio structure (possibly connected to young radio sources). The higher specific star-formation rate for these galaxies suggests that the HI absorption may be largely due to star-forming gas in their hosts.

The presence of obscuring structures in the circumnuclear regions can also be explored by comparing the detection rates of HI absorption in type-2 (in this case radio galaxies) and type-1 (i.e. quasars) radio AGN. A group of objects for which this has been done are the young radio sources, such as compact steep spectrum (CSS) and gigahertz peaked spectrum (GPS) sources (Figs. 10, 11). The general properties of the HI absorption in these objects will be discussed in Sect. 4.2.3, but in the context of studying the effects of orientation and obscuration, it is interesting to note that CSS/GPS objects classified as radio galaxies have an HI detection rate (∼40%) significantly higher than the detection rate (∼20%) observed towards CSS/GPS quasars (Gupta et al. 2006; Gupta and Saikia 2006). Similarly, from a study of 49 GPS and CSS sources, Pihlström et al. (2003) find that HI absorption is more likely to arise in objects classified as galaxies, rather than in quasars. This is expected if most of the HI is distributed in a circumnuclear structure that is obscuring a type-2 AGN (i.e. radio galaxies), while type-1 AGN (i.e. quasars) are unobscured. The situation seems to be different for red quasars. These objects have shown higher detection rates of HI absorption (Carilli et al. 1998b; Yan et al. 2016), consistent with these sources likely being in a crucial, early phase of their lives when the AGN emission is still obscured by gas and dust (see also Sect. 5.3).

As a final remark, it is interesting to note that, as for Seyfert galaxies, the conditions of the gas close to a more powerful AGN ($r <$ few tens of pc) are strongly affected by the presence of the AGN. The presence of circumnuclear disks and tori can be traced by ionised, atomic neutral and molecular gas. Warm ionised gas can be traced by free–free absorption, while the hot ionised gas can be identified by Compton thick structures (see,

e.g. Risaliti et al. 2003; Ursini et al. 2018). The confirmation of the presence of largely ionised gas (likely distributed in a rotating structure) in the immediate proximity of the AGN and, consequently, of a "central hole" (inside $\sim$ 2 pc) of atomic gas, has been confirmed by the combination of free–free and HI observations in a few cases. One of the best studied objects where the observations have shown that these structures are actually present, is the nearby galaxy NGC 1052 (Vermeulen et al. 2003b) but other examples with similar properties will be discussed in Sect. 4.2.2.

4.2.2 Evidence of disks and tori from VLBI observations

The final test to pin down the properties of circumnuclear-disks and tori is to spatially resolve them and trace the kinematics of the gas. Such studies require extremely high (i.e. milli-arcsecond) spatial resolution which can be reached using VLBI observations. This can be done in the cases where the structure and extent of the radio continuum on such small scales provides a large enough screen so that the overall kinematics of the absorbing gas can be reconstructed. A useful compilation of VLBI and VLBA HI observations published up to 2010 is presented in Araya et al. (2010). Some more publications have appeared since and will be described below.

One of the first sources where the HI absorption was attributed—already from low spatial resolution observations—to a circumnuclear absorbing structure was the prototype FR-II radio galaxy Cygnus A (Conway and Blanco 1995). The large width of the HI absorption profile (379 ± 62 km s^{-1}) from the nuclear region and the offset from the systemic velocity argue against the absorption arising at large (kpc-scale) distances from the nucleus because one would expect the profile to be much narrower and centred on the systemic velocity. Instead, the large line width indicates the absorption is produced by a geometrically thick torus or a circumnuclear disk close to the active BH, since the velocity of the torus/disk must be comparable to the orbital velocity in this case. This scenario was confirmed by VLBA observation of Cygnus A (Struve and Conway 2010). The data showed that the HI absorption comes from a region perpendicular to the radio axis and as well as from the counter jet. This is exactly what one would expect for a nuclear disk. A velocity gradient over the absorbing region was seen, as illustrated in Fig. 12. From these data one can estimate that the HI absorbing gas lies at a radius of $\sim$ 80 pc and that the disk has a scale height of about 20 pc, density $n > 10^4$ cm^{-3} and a total column density in the range 10^{23}–10^{24} cm^{-2} with $T_s < 740$ K.

Even in a powerful radio galaxy like Cygnus A, the counter-jet is only just bright enough for what is needed for detecting HI absorption. This is why detailed studies of HI absorption using VLBI data have been done for only a limited number of extended sources, some of them low-power radio galaxies. The best examples are NGC 4261 (van Langevelde et al. 2000, see Fig. 13), Hydra A (Taylor 1996) and Centaurus A (Espada et al. 2010). In the first two objects, the evidence for a nuclear disk is based on the fact that the HI absorption is relatively broad (~ 80 km s^{-1}) for the small background source (< 10 pc) sampled by the VLBI data. In Hydra A, the torus/disk could be quite edge-on, allowing to estimate the vertical extent ($\sim$ 30 pc). In NGC 4261, the HI absorption is detected against the counter-jet (see Fig. 13 taken from van Langevelde et al. 2000) at only 6 pc from the nucleus. For Centaurus A, the

VLBA observations of Espada et al. (2010) have explored the pc-scale inner regions and identified a number of narrow absorption components seen along the jet, and a broader (~ 50 km s^{-1}, also detected by Sarma et al. 2002) HI line which is more prominent towards the central and brightest 21 cm continuum component, base of the nuclear jet but not the nucleus itself, i.e. at a radius of ~ 20 mas (or 0.4 pc) further from the nucleus. Whether this component is part of the circumnuclear disk described in Sect. 4.2 still needs to be confirmed. Another FR I radio galaxy, the giant NGC 315, has been studied in detail with VLBI focusing on the role of HI for the fuelling process (see Sect. 6).

As mentioned above, a group of sources that is suitable for VLBI observations are the young as well as restarted radio galaxies. In these objects, the radio continuum typically extends on scales of a few hundred pc to about a kpc and this offers the best background for tracing the complex distribution and kinematics of the multiple structures that can be present.

In the case of the restarted radio galaxy 3C 293, at least two structures with different velocity widths, both having large-scale velocity gradients, are seen against the kpc-sized continuum (Beswick et al. 2004). One is seen against the eastern radio jet co-spatial with the location of dust lanes observed by the HST and which has a small velocity gradient of ~ 50 km s^{-1} arcsec^{-1}, consistent with the velocity gradient observed for the ionised gas. The second structure, with possibly a larger velocity gradient, could be due to a circumnuclear disk on scales of ~ 400 pc. Also in the restarted, giant galaxy 3C 236 (see Tremblay et al. 2010 for an overview of its properties) a velocity gradient is observed which, also in this case, seems to correspond to the dust-lane, the ionised gas disk and the molecular gas disk. Clouds of HI are also detected with masses of a few $\times 10^4$ $M_\odot$ (see Struve and Conway 2012, recently confirmed by Schultz et al. submitted). In both 3C 236 and 3C 293 the overall distribution and kinematics of the gas is complicated by the presence of fast HI outflows, see Sect. 5.1.

The groups of objects most commonly studied in VLBI are the CSS and GPS radio galaxies. The HI absorption in these objects appears to trace a variety of absorbing structures (including infalling and outflowing gas), but a number of these radio galaxies have also shown, on pc-scales, HI distributed in torus-like structures with evidence of rotation.

One of the best examples is 4C 31.04. In this compact, double-lobed radio galaxy, a sharp edge in optical depth has been observed against the western lobe, while for the eastern lobe the opacity is quite uniform (Conway 1996; Struve and Conway 2012). This has been taken as a signature of an almost edge-on torus/disk which extends to radii $r < 200$ pc. HST observations of 4C 31.04 (Perlman et al. 2001) have confirmed the presence of a dust disk of the dimensions as derived from the HI absorption.

Another example is the compact, double-lobed radio galaxy, PKS 1946+708, where HI absorption was detected towards the entire ~ 100 pc extent of the continuum source (Peck et al. 1999; Peck and Taylor 2001). The absorption against the core is broader (~ 300 km s^{-1}), but has lower optical depth than the absorption against the rest of the source (see Fig. 9 and Peck and Taylor 2001 for details). According to Peck and Taylor (2001), this is in agreement with the thick torus scenario in which gas closer to the central engine rotates faster and is much warmer, thus lowering the optical depth. The

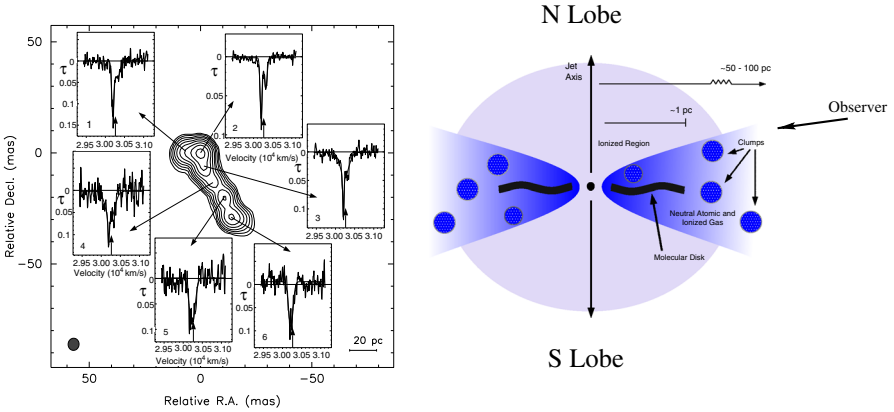

Fig. 9 Left: H I absorption profiles toward the radio source PKS 1946 + 708 overlaid on the 1.3 GHz continuum contours. Right: Cartoon illustrating the possible distribution of the gas along the tine of sight to the jet components. Images reproduced with permission from (left) Peck and Taylor (2001), copyright by AAS; (right) from Morganti et al. (2004), copyright by Elsevier

narrow lines are explained as coming from gas further out in the torus, possibly related to an extended region of higher gas density and having a diameter of the order of at least 80–100 pc. In an other double-lobed radio galaxy, B2352 + 495, H I absorption with a width of ~ 100 km s^{-1} has been found located against the core, and tentatively showing a velocity gradient perpendicular to the jet direction (Araya et al. 2010). Also for this case, a component tracing circumnuclear material is suggested to cause the absorption. In addition, a very narrow and redshifted (about 130 km s^{-1}) absorption is detected and likely tracing an infalling cloud at larger distance from the nucleus.

Finally, in PKS 1814-637, a radio source $\sim$400 pc is sized and a rare example of a powerful radio source hosted by a disk galaxy, one can identify at least two separate disks producing the H I absorption (Morganti et al. 2011). The deep absorption seen in this object likely originates from cold gas located at large distances from the nucleus and is probably associated with the large-scale disk (which has a thickness of 400–500 pc) of the host galaxy. A shallower, broader component could, instead, trace a circumnuclear disk located closer to the radio source (and having a thickness of the order of 100 pc). The large width of the shallow, shifted absorption features would be due to unresolved rotation projected along the line of sight. The VLBI observations are confirming the presence of circumnuclear structures containing H I, likely playing an important role in the fuelling of the SMBH.

Most VLBI studies are based on sources having redshifts up to $z \sim 0.12$, corresponding to the frequency of the redshifted H I to be larger than 1270 MHz. This frequency represents the limit of the receivers of many of the VLBI/VLBA antennas. Being restricted to very low redshifts is one of the major limitations for the high-resolution study of the properties of H I in radio galaxies. For a few years, a number of antennas which are part of the European VLBI Network (EVN) were equipped with UHF receivers covering the frequency range 800–1300 MHz. This has allowed to reach redshifts up to $\sim$ 0.8 and to explore the H I absorption in a number of more

distant sources, albeit the relatively poor sensitivity of these receivers has limited the observations to bright sources. Examples are the compact, double-lobed radio galaxies 2050 + 364 ($z = 0.35$; Vermeulen et al. 2006), 3C 49, and 3C 268.3 ($z = 0.62$ and $z = 0.37$ respectively; Labiano et al. 2006). Also in these objects the VLBI data show a variety of situations. In 3C 49 and 3C 268.3, the radio lobes against which the absorption occurs are brighter, are closer to the core and, in the case of 3C 268.3, are more depolarised. The observed asymmetries suggest that the H I gas is involved in an interaction with the radio plasma. In 2050 + 364, like in some of the objects described above, two absorption systems—one very narrow and one shallow and broader—have been found. The narrow component covers the entire source, perhaps indicating that also in this case the origin is gas at larger distances from the core. The origin of the broad absorption is more difficult to establish, because of a difference between the redshift derived from the optical emission lines ([O III] and Hβ, Vermeulen et al. 2006).

4.2.3 Nuclear structures in young radio galaxies

The detection rate, column density and line width of H I absorption in radio galaxies appears to depend on the characteristics of the sources. For studying H I absorption, intrinsically compact radio sources like GPS and CSS have gained particular attention. These sources are considered to be recently born (or re-born) radio AGN, although their properties may also be the result of a strong effect of the surrounding ISM.

A number of studies have shown that these compact sources, compared to more extended ones, have a higher detection rate of H I absorption, reaching 40–45% (Véron-Cetty et al. 2000; Vermeulen et al. 2003a; Pihlström et al. 2003; Gupta et al. 2006; Chandola et al. 2011; Geréb et al. 2015). Interestingly, although the statistics is not as good, such a high detection rate is also observed for restarted radio galaxies, where a newly born radio source is embedded in a large, much older object (see the cases of 3C 236 Mirabel 1989; Morganti et al. 2005a; CTA 21 Salter et al. 2010; 3C 321 and 4C 29.30 Chandola et al. 2010, 2012; 4C 12.50 Morganti et al. 2013 and Saikia et al. 2007 for some examples). The H I absorption detected in CSS/GPS and restarted sources has also been found to trace gas with higher column density compared to extended radio sources, and the spectra more often indicate gas with disturbed kinematics, traced by the asymmetric, often highly blueshifted profiles (Geréb et al. 2015; Glowacki et al. 2017 see also Fig. 10).

The high detection rates could suggest that these radio sources are, on average, more often embedded in a rich ISM. This would have implications for the impact these AGN may have on the surrounding medium which, in turn, may be important for the role of AGN feedback in galaxy evolution (see Sects. 4.2.3 and 5.1). Pihlström et al. (2003) have found an anti-correlation (albeit with a large scatter) between the source linear size and the H I column density. They derive a relation $N_{\rm H\,I} = 7.2 \times 10^{19} L^{-0.43}$ cm^{-2}, with L the linear size in kpc, using the data from their survey (see also Vermeulen et al. 2003a). The explanation put forward by these authors is that the relation is probing a surrounding medium whose density decreases with radial distance from the centre. Under reasonable assumptions, a spherical distribution of the absorbing gas

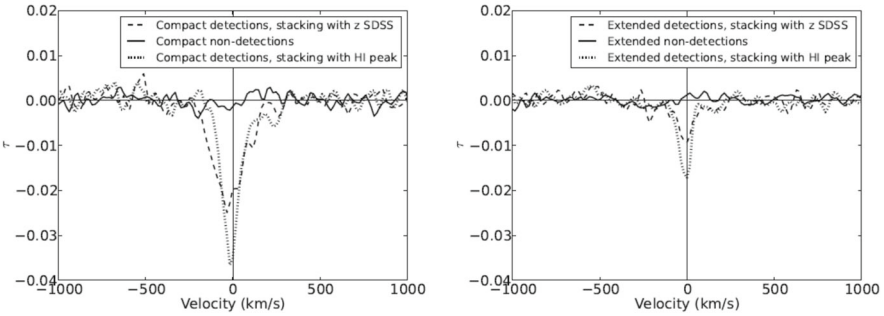

Fig. 10 Stacked H I profiles for compact (left) and extended (right) sources. The profiles show the higher optical depth and the broader width of the stacked profiles of the former, suggesting differences in the medium in which the two groups of objects are embedded. Both panels show that for both compact and extended sources, even if a large number of spectra are stacked of sources where no absorption was detected in the individual spectra, the stacked spectrum still does not show a detection, indicating that a population of gas-poor galaxies exists and/or where the conditions of the H I (e.g. spin temperature) are different. Image reproduced with permission from Geréb et al. (2014), copyright by ESO; see also Morganti et al. (2015a)

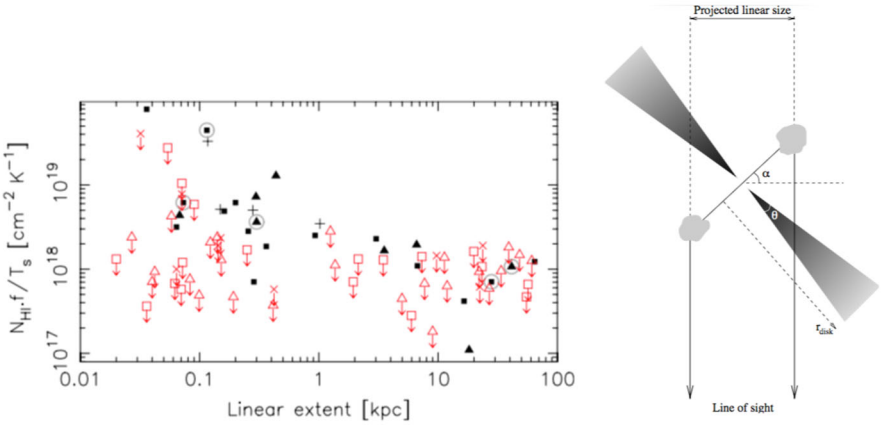

Fig. 11 Left: scaled velocity integrated optical depth ($1.823 \times 10^{18} \tau dv$) of the H I absorption vs. the linear extent of the radio source size. Black symbols are detections while red symbols are upper limits. Right: cartoon of the possible geometry of the disk structure producing the H I absorption in CSS/GPS sources. Images reproduced with permission from (left) Curran and Whiting (2010), copyright by AAS; and (right) from Pihlström et al. (2003), copyright by ESO

does not produce the observed relation. A better model is a disk-like gas distribution in a plane roughly perpendicular to the radio source and with opening angle of 20°. However, this explanation (described by the cartoon in Fig. 11 right) is likely not the full story. The continuum morphology of CSS/GPS sources is not always this symmetric, the disk itself is likely not necessarily uniformly filled and is not always perpendicular to the radio source axis. Furthermore, Fig. 11 (left) shows the integrated optical depth vs. linear size for all objects (i.e. not only CSS/GPS) collected by Curran and Whiting (2010), including the upper limits. It can be seen that, deviations from the correlation do exist. For example, for a sample of high-frequency peakers (HFP),

which are extremely small sources (i.e. with linear sizes $\leq$ 20 pc) and considered to be radio AGN in their very first stages of evolution, only a low fraction of HI absorption detections was found (see Orienti et al. 2006). This is at odds with the expectations from the above relation for such small scales, where high HI column densities ($\geq 10^{21}$ cm^{-2}) would have been expected. On the other hand, and because of the small sizes of the sources, these findings could be explained if the line of sight is passing mainly through the inner regions of the disk where the gas is likely to be mostly ionised, as discussed above. The correlation may also be affected by the limited sensitivity of some of the HI absorption observations. For example, in the case of the "baby" source PKS 1718–63 having a size of only 2 pc (see Véron-Cetty et al. 2000; Maccagni et al. 2014, more in Sect. 6), two narrow absorptions with $N_{\rm HI} = 7 \times 10^{17} T_{\rm s}/c_{\rm f}$ cm^{-2}. This is lower than expected from the anti-correlation between the source linear size and the HI column density for a source of such a small size (see Fig. 11).

An alternative explanation for this anti-correlation has been put forward by Curran et al. (2013a) who suggested that the higher detection rate in compact objects could result if the size of the sources and the size of the absorbers are very similar. This would indicate that the typical cross section of cold absorbing gas is of the order 100–1000 pc. They remark on the possibility that the correlation is then the by-product of indirect relations between the column density and the covering factor which in turn is suggested to be related to the source size. The large scatter in the correlation suggests that, although this can affect the correlation, it is unlikely that this effect applies to every source.

Despite the high detection rate of HI absorption and the high column densities observed, it is interesting to note that among compact/young objects, and the same is true for extended radio sources, there is a population that appears to be poor in HI. This is shown in Fig. 10, taken from Geréb et al. (2014), where the stacked spectra are shown for compact (left) and of extended (right) sources. The result from the stacking of non-detections is indicated, in both plots, by a solid line. It can be seen that, even if a large number of spectra of such non-detections are stacked, no HI absorption is seen even among the compact sources, Fig. 10 (left). It appears, therefore, that there is a significant group of galaxies where either there is little HI, or in which the conditions of the gas are different, for example, that the spin temperature is higher. Orientation effects play a role, but does not seem to be fully able to explain the effect (Maccagni et al. 2017). To further study this, Maccagni et al. (2017) have stacked the central emission spectra of the those early-type galaxies from the ATLAS^{3D} sample that were undetected in emission and found a detection of HI emission equivalent to a column density of $N_{\rm HI} \sim 2.1 \times 10^{19}$ cm^{-2}. This is quite low, confirming the presence of a population of early-type galaxies with genuinely a limited amount of HI. HI at these low column densities likely has $T_{\rm s}$ well above 100 K (Kanekar et al. 2011) which makes it even harder to detect these low column densities in absorption. Indeed, the limits reached by the stacking of HI absorption spectra discussed above is not yet low enough to detect such columns in absorption and this is one of the tasks for the future large surveys.

4.3 H I absorption in galaxy clusters

Some of the radio galaxies where H I absorption has been found (e.g. Hydra A and Cygnus A) are located in the centre of a galaxy cluster. Cold gas is now often detected in clusters, in particular, thanks to the improved sensitivity and resolution provided by ALMA. This is especially the case in the central regions of cool-core clusters (see, e.g. Edge 2001; Salomé et al. 2006; Russell 2017 and refs. therein). In some cases, the detected molecular gas is extended and likely represents the end product of hot gas lifted by the radio jets and cooling rapidly as result of instabilities.

The information on H I absorption in cluster galaxies is still limited and heterogeneous. As a result, very little is known about to what extent the observed properties depend on the dynamical state of a cluster or whether H I absorption more often in, for example, cool-core clusters. The only attempt of a more systematic study of H I absorption in clusters has been done by Hogan (2014). This has addressed the presence of H I absorption in samples (albeit small) of bright central galaxies in clusters. In general, this study finds that many H I absorption profiles of galaxies in clusters show the presence of a narrow (often redshifted) absorption line and of a broad absorption component at the systemic velocity. The absorptions tend to have column densities covering a not too broad range, i.e. $N_{\rm H\,I} < 3.0 \times 10^{21}$ cm^2, for $T_{\rm s}$= 100 K. Following Hogan (2014), the findings are broadly consistent with the majority of the broad absorptions being attributable to a central toroidal structure and the narrower components due to infalling clouds on their way to feed the AGN or to replenish the torus.

A number of studies focusing on single objects are also available. H I absorption has been detected against the central radio galaxy of large clusters, for example in Abell 2597 (PKS2322-123, see O'Dea et al. 1994; Taylor et al. 1999), in the Perseus cluster (3C 84/NGC1275, Sijbring et al. 1989; Jaffe 1990 and refs. therein), in Abell 1795 (4C 26.42, van Bemmel et al. 2012), and in Abell 407 (4C 35.06, Shulevski et al. 2015). In addition, other cases of absorption in cluster galaxies are known like PKS 1353-341 (Véron-Cetty et al. 2000), Hydra A (Taylor 1996) and Cygnus A (Conway and Blanco 1995; Struve and Conway 2010). For some of these objects, high spatial resolution, VLBI observations are also available giving more detailed information on the structure of the absorber (see Sect. 4.2.2 for more details).

In the extreme case of NGC 1275 in the Perseus Cluster, two absorbing systems have been found, at very different velocities. The so-called high velocity system (discovered by De Young et al. 1973) is a relatively narrow H I absorption line redshifted $\sim$3000 km s^{-1} from the systemic velocity of NGC 1275. Based on optical narrow-band images (Lynds 1970) and recent VLA observations (Momjian et al. 2002), this system is likely caused by a foreground galaxy, projected onto NGC 1275. The low velocity system (discovered by Crane et al. 1982 and studied in some detail by Sijbring et al. (1989); Jaffe (1990) is, instead, centred on the systemic velocity of NGC 1275, at 5300 km s^{-1}. This absorption is broad, with FWHM $\sim$500 km s^{-1} (Jaffe 1990), larger than what is typically found in radio galaxies outside clusters.

The case of PKS 2322-12 in the Abell 2597 is similar (Taylor et al. 1999). At low spatial resolution, the H I absorption shows a broad and a narrow velocity compo-

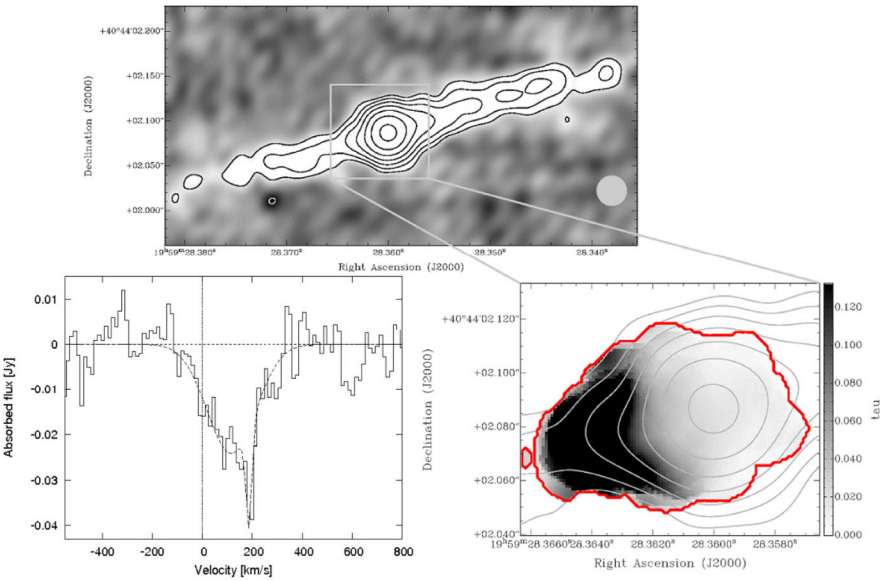

Fig. 12 Top panel: continuum image of the nuclear jets of Cygnus A at 1340 MHz. The lowest contour is at 2 mJy beam^{-1} with subsequent contours increasing by factors of 2. The effective beam FWHM (see Sect. 2) is indicated in the lower right corner. Bottom-left panel: integrated absorption spectrum from the blanked cube with the velocities shifted to the rest frame of Cygnus A. The dashed line shows the two component Gaussian fit. Bottom-right panel: contours show continuum. Grayscale shows the mean opacity over the rest frame velocity range -80 to $+170$ km s^{-1}. The thick dark line shows the un-blanked region over which the integrated absorption spectra (shown in the bottom left panel) is calculated. Image reproduced with permission from Struve and Conway (2010), copyright by ESO

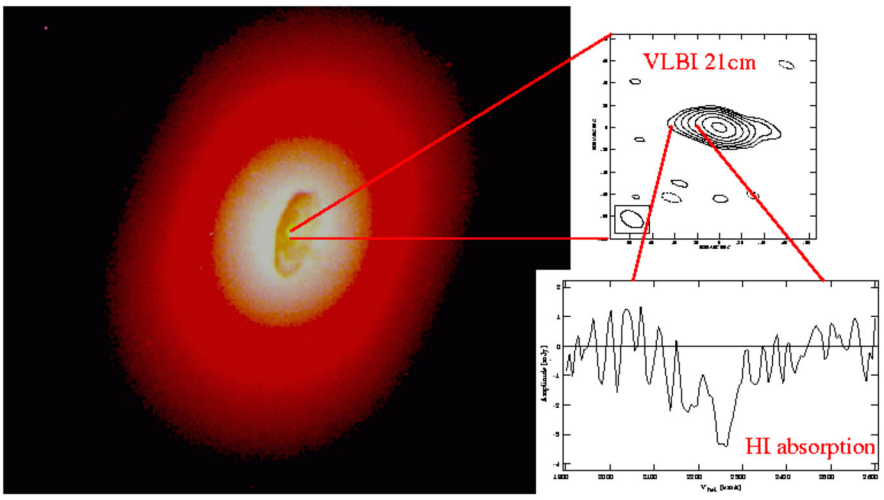

Fig. 13 The background represent the HST image of NGC 4261. The inset are the VLBI images (from van Langevelde et al. (2000)) of the nucleus at 21 cm (right) and the HI absorption spectrum observed slightly offset from the nucleus (left). Courtesy of Huib Jan van Langevelde

nent (O'Dea et al. 1994). Using VLBI, Taylor et al. (1999) showed that the narrow component is seen against both jets and against the nucleus, whereas the broad component is observed only against nucleus. They interpreted the broad component as a circumnuclear torus and the narrow component as inward streaming (cold) gas. This has been recently confirmed by the study of the molecular gas with ALMA, which finds a similar kinematics (Tremblay et al. 2016).

Thus, studies of H I absorption in cluster galaxies, although they are still sparse in number, can provide complementary information to the molecular gas to complete the picture of the gas in these complex environments.

5 Absorbing structures: fast outflows and kinematically disturbed H I gas

Perhaps the most surprising result in recent years in the field of H I absorption has been the discovery of fast (> 1000 km s^{-1}) AGN-driven outflows of atomic hydrogen. Such outflows were identified through the discovery of very broad, blueshifted and typically shallow absorption wings in the spectra of active galaxies. Such velocities are much larger than typical rotational velocities and thus cannot be associated with rotating gas structures. The fact that these fast components are blueshifted relative to the systemic velocity clearly implies that the absorbing gas is outflowing. No redshifted components of similar widths have been detected so far (see also Sect. 6).

AGN driven gas outflows are one of the manifestations of the effects of AGN on the gas surrounding them. They are a key component in current models of galaxy evolution because of their suspected role in regulating star formation as well as the growth of the central super massive black hole. The presence of H I (and also cold molecular gas) in such outflows is perhaps counter-intuitive because of the large amounts of energy emitted by the AGN. The origin of the atomic gas (and more in general of the cold gas) associated with outflows is still a matter of debate. The preferred explanation appears to be that this cold gas is the result of in situ fast cooling after the gas has been shocked and accelerated (e.g. Mellema et al. 2002; Fragile et al. 2004), but the possibility of pre-existing gas being accelerated has also been put forward (see Sect. 8 for more details). Outflows of ionised gas have been known for a long time to be relatively common in AGN (Tadhunter 2008; King and Nixon 2015). However, the discovery of the role of the H I (and molecular gas) in these phenomena has broadened our view of AGN and of the conditions of the gas around them. All phases of the gas take part in the outflows, and therefore, to get the full picture of their physical properties, multi-wavelength observations are needed, including those of H I (see e.g. Morganti 2017).

5.1 Occurrence of fast H I outflows

The discovery of the fast H I outflows has been possible due to the larger instantaneous observing bandwidths (covering at least several thousands of km s^{-1}, see, e.g. Fig. 14 left) and the better spectral stability which have both become available as result

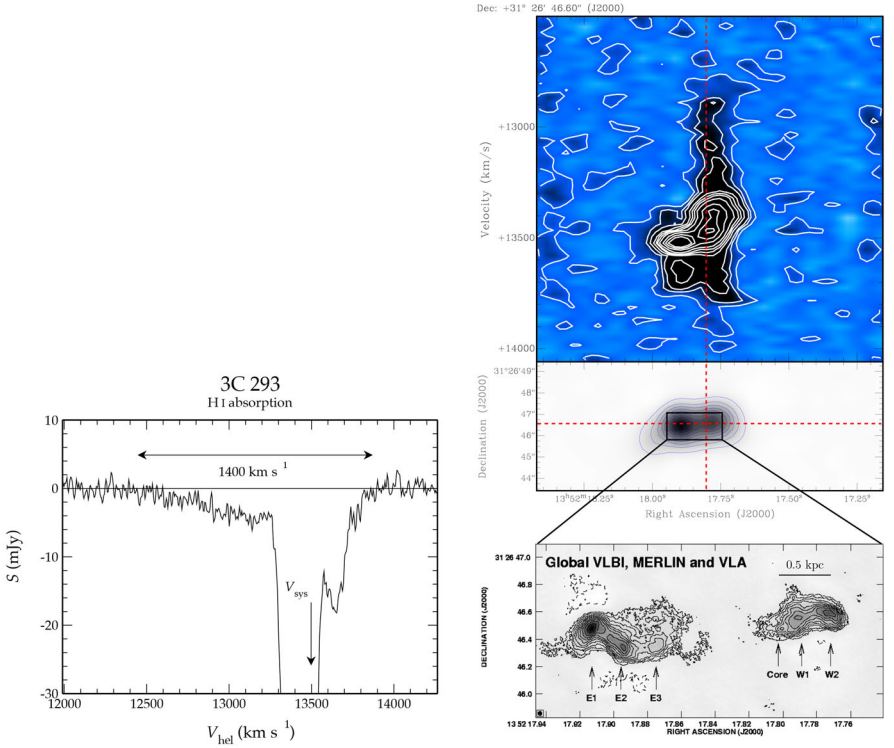

Fig. 14 Left: Integrated H I absorption profile obtained from the WSRT showing a very broad, blueshifted wing, indicating a fast H I outflow, in addition to the deep absorption profile near the systemic velocity due to the large-scale gas disk in the object. Right Top: Position–velocity diagram extracted along the radio axis of the continuum source of 3C293 as obtained with the VLA, showing that the outflow is associated with the western lobe of this radio galaxy. Middle: The continuum image of 3C293 from these VLA observations with a resolution of $\sim$ 1 arcsec. The horizontal red line marks the axis along which the position–velocity diagram was extracted while the vertical red line indicates the position of the core as determined from the VLBI image in the bottom panel. Bottom: the combined 1.4 GHz global VLBI, MERLIN and VLA image of the central regions of 3C293 (from Beswick et al. 2004). Images reproduced with permission from (left) Morganti et al. (2003), copyright by AAS; and (right) Mahony et al. (2013), copyright by the authors

of upgrades of several radio telescopes. Earlier observations failed to detect these fast outflows, partly because the velocity range covered was simply not large enough, and partly due to lack of sensitivity and/or stability. However, some indications for the AGN having an effect of the surrounding ISM had been found earlier as, for example, in the study by Vermeulen et al. (2003a) of a sample of CSS/GPS in which the prevalence of blueshifted absorption in the H I profiles was already emphasised, although the widths of these blueshifted components were smaller than those of the fast outflows found later.

Since the first discovery of a fast H I outflow (Morganti et al. 1998, 2003, see Fig. 15), a growing number of cases have been reported. A summary of the H I outflows known so far is given in Table 1. Studies of H I outflows have focused on three main issues: the occurrence of fast outflows, the localisation and physical parameters of the

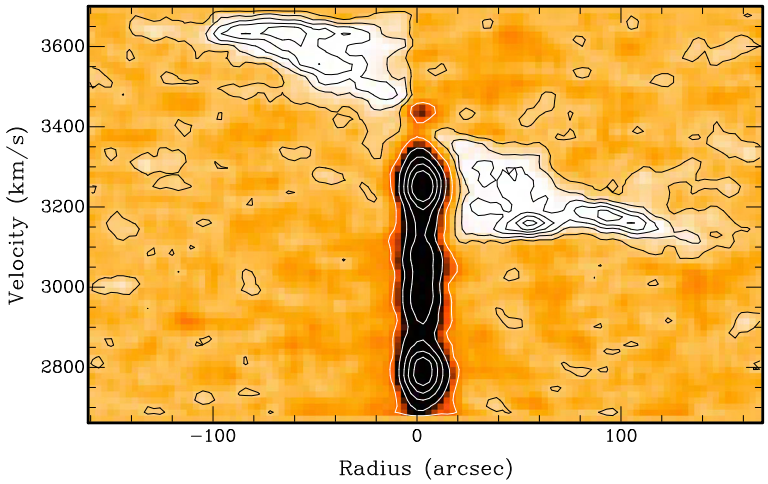

Fig. 15 The position–velocity plot from the ATCA HI data of IC 5063 taken along the axis of the radio jet showing the first fast HI discovered (Morganti et al. 1998). The black contours represent the HI emission coming from the large-scale, rotating HI disk of IC 5063 and indicate the range of velocities associated with normal rotation. The grey contours represent the absorption due to the HI outflow and show that the blueshifted velocities of the outflowing gas extend to well outside the velocity range of the regularly rotating gas

outflows, and the mechanisms driving them. Fast HI outflows can only be observed using HI absorption due to the fact that, so far, these outflows appear to be limited to the central kpc, meaning they have an apparent size of at most one arcsecond. The column density sensitivity of current (and future) radio telescopes is insufficient for detecting the emission from these outflows at the required resolutions (as described in Sect. 2.4).

An example of one of the first HI outflows detected in a radio galaxy is 3C293, shown in Fig. 14. On the left is shown the integrated absorption profile detected against the unresolved central radio source of this object, using the WSRT (Morganti et al. 2003). The profile shows the broad blueshifted wing with velocities which clearly exceed the velocity range of the regularly rotating gas disk indicated by the extent of the deep absorption. The large blueshift of the wing is an unambiguous signature that the gas is outflowing. The position–velocity diagram from higher spatial resolution observations (VLA, ~ 1 arcsec resolution, Mahony et al. 2013) shows that much of the outflow is occurring against the western radio lobe of 3C293 which implies that the outflow extends to at least 0.5 kpc from the nucleus.

The only attempt done so far to quantify how common HI outflows are has been based on the survey presented in Geréb et al. (2015) and Maccagni et al. (2017). Of the galaxies detected in HI absorption, at least 15% show fast outflows which, given the overall detection rate of HI absorption of 30% in their sample, translates to about 5% of all radio sources having fast outflows. This is a lower limit because of the limited sensitivity of the survey, but also because not every outflow will be located in front of the radio continuum and will not be detected in absorption. From the above survey, but also from other studies (e.g. Morganti et al. 2005a;

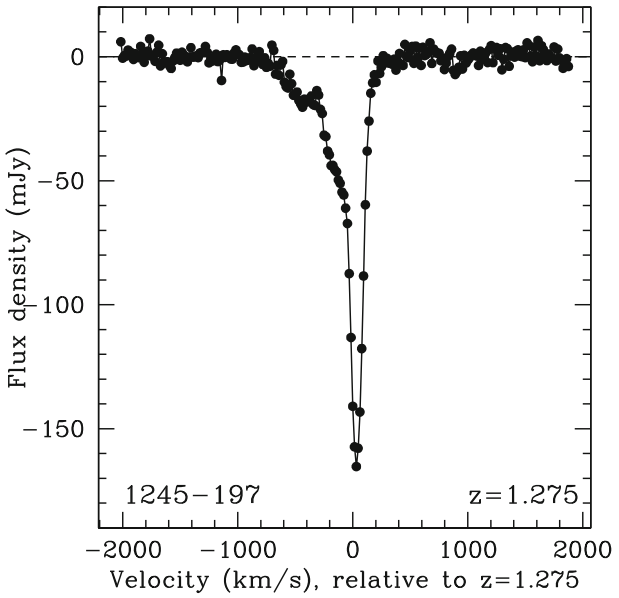

Fig. 16 The GMRT HI 21 cm absorption spectrum towards TXS 1245-197 at $z = 1.275$, showing a broad, blueshifted component extending more than 800 $\mathrm{km\,s^{-1}}$. Image reproduced with permission from Aditya and Kanekar (2018), copyright by the authors

Aditya and Kanekar 2018, and references therein), it is now clear that in particular young radio galaxies, as well as restarted radio galaxies, are the objects where HI outflows are more likely to occur. This is expected given the small sizes of such radio sources and their dense ISM. Interestingly, the highest redshift outflow observed so far (from Aditya and Kanekar (2018), see Fig. 16) is also found in a GPS source.

In addition, a possible correlation between the velocity of the outflow and the radio power of the AGN has been found (Maccagni et al. 2017). This is consistent with the observation that most of the HI outflows are found among relatively high-power radio sources (Geréb et al. 2015; 4C 31.04 from the WSRT Morganti et al. in prep.). However, also low-power radio sources can provide a driver for gas outflows and examples are NGC 1266 (Alatalo et al. 2011; Nyland et al. 2013) NGC 1433 (Combes et al. 2013), IC 5063 (Oosterloo et al. 2000) and Mrk 231 (Morganti et al. 2016). Interestingly, these objects are commonly classified as radio-quiet objects, but IC 5063 is now nevertheless one of the best cases known showing the relevance of the jet for driving the outflow.

Interesting are also the results derived from HI absorption for interacting and FIR-bright galaxies and ULIRG objects. A high fraction of HI outflows (with velocities exceeding 1500 $\mathrm{km\,s^{-1}}$ in some cases) have been found using the GBT in nearby ULIRGs and quasars studied by Teng et al. (2013). Very intriguing is that they find polarisation-dependent HI absorption which they attribute to absorption of polarised continuum emission by foreground HI clouds. This result still needs confirmation from interferometric observations.

5.2 Location and other parameters of the H I outflows

In a (unfortunately still limited) number of cases, the spatial resolution of the data is insufficient to determine the location of the outflow. The first object where an H I outflow was discovered is the Seyfert 2 galaxy IC 5063 (Morganti et al. 1998). This object is one of the few Seyfert galaxies with relatively strong radio continuum. The radio morphology shows a core and two lobes, one of which is ending in a particularly radio bright hot spot, about 500 pc from the nucleus. In this galaxy, highly blueshifted absorption ($\sim$ 700 km s^{-1}, see Fig. 15) was detected using the ATCA. The spatial resolution of these ATCA data were not sufficient to determine the location of the outflow, but later VLBI observations allowed to establish that the location of the fastest part of the outflow is coincident with the bright hot spot mentioned above, around 0.5 kpc from the nucleus (Oosterloo et al. 2000). This observation was the first indication that the jet, and not the central source, could play a role in driving a fast H I outflow. Later observations of the molecular gas in this object have shown that, although the fastest outflow occurs at the bright hotspot at the end of the jet, the region with outflowing gas exactly coincides with the entire radio jet, reinforcing the idea that the jet is driving the outflow (see also Sect. 8).

Also in the case of 3C 293 (see Fig. 14 right), the strongest outflow of $\sim$ 1000 km s^{-1} is seen against the western inner radio lobe, about 0.5 kpc in size (Morganti et al. 2003; Mahony et al. 2013). Similarly, the outflow observed in 3C 305 is located about 0.5 kpc from the core (Morganti et al. 2005b). A very convincing example for the outflows being off-nucleus is the case of 4C 12.50, a young (possibly restarted, see Stanghellini et al. 2005), IR-bright radio galaxy. In this object, the fast outflow H I has been found to be located at the end of a radio lobe, and is wrapped around a bright hot spot in this lobe (Morganti et al. 2013, see Fig. 17).

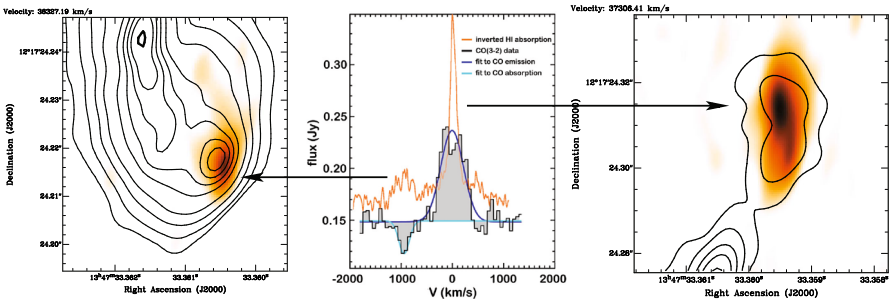

Fig. 17 The distribution of the H I absorption (orange–white) in two velocity channels for the source 4C 12.50, superimposed to the continuum emission (contours) showing the location of the two H I clouds detected in absorption (from Morganti et al. 2013). The inverted integrated H I absorption profile is shown in the central panel and clearly shows a strong, blueshifted H I outflow of $\sim$ 1000 km s^{-1} (from Morganti et al. 2005a). The cloud shown in the right panel has a narrow absorption profile near the systemic velocity, while the left panel shows the location of H I absorption associated with the fast H I outflow, co-spatial (in projection) with the bright radio hot spot. Also shown is the CO profile (taken from Dasyra and Combes 2012 which shows that a very similar outflow is detected in CO absorption. Image reproduced with permission from Morganti et al. (2013), copyright by AAAS

Thus, in a significant number of cases, the spatial coincidence of the outflow with bright, non-nuclear continuum features suggests that the outflow likely originates from the interaction between the expanding radio plasma and the ISM. This is in agreement with what is now predicted by numerical simulations (Wagner and Bicknell 2011; Wagner et al. 2012; Mukherjee et al. 2016, 2018a). Such simulations describe the effects of a newly formed radio jet trying to find its way through a dense and clumpy gaseous medium. Such a porous medium with dense clumps forces the jet to find the path of least resistance. While doing so, the jet interacts with, and gradually disperses, the dense clouds away from the jet axis, forming a turbulent cocoon of over-pressured gas. In this way, clouds can be accelerated to high velocities and over a wide range of directions, not only in the direction of the jet movement, but also away from the jet axis.

However, not in every radio source the jet is the main driver of the outflow. For example, in the case of Mrk 231 an HI outflow is present which reaches velocities up to 1300 $\mathrm{km\,s^{-1}}$ blueshifted compared to the systemic velocity and which has properties very similar to outflows found in other radio galaxies. However, the energetics of the radio source, and the lack of a clear kpc-scale jet, suggest that the most likely origin of the HI outflow is a wide-angle nuclear wind, as earlier proposed for this object to explain the neutral outflow traced by Na I and by molecular gas. This suggests that different mechanisms can produce an HI outflow, similarly to what is found for other phases of the gas (see Sect. 8, see also Tadhunter et al. 2014).

The mass outflow rate is an important parameter to be able to judge the impact the outflow may have on the host galaxy. The estimate of this parameter can be quite uncertain, in particular, if we do not have location and extent of the HI outflow. This is in any case always limited by the size of the radio continuum, which can be smaller than the scale of the outflow, setting a lower limit to the outflow rate derived. The HI mass outflow rate can be estimated following Heckman (2002) and Rupke et al. (2002):

$$\dot{M} = 30 \cdot \frac{\Omega}{4\pi} \cdot \frac{r_*}{1\,\mathrm{kpc}} \cdot \frac{N_{\mathrm{HI}}}{10^{21}\,\mathrm{cm^{-2}}} \cdot \frac{v}{300\,\mathrm{kms^{-1}}}\, M_\odot\,\mathrm{yr^{-1}} \tag{7}$$

and for the known cases is listed in Table 1. Here it is assumed that the gas is flowing at a velocity equal to the FWZI/2 of the blueshifted component, at an observed radius r_* and into a solid angle Ω assumed to be π steradians.

The mass outflow rates of the HI outflows range between a few and a few tens $M_\odot\,\mathrm{yr^{-1}}$ (see Table 1). For radio galaxies the number of outflows known is sufficient to draw some statistical conclusions and their HI outflow rates typically appear to be higher than those associated with the outflow of ionised gas. For the very few objects where this comparison can be done directly, the outflow rate of the HI outflow appears to be lower (or at most comparable) with those derived for the molecular gas, but such comparisons will need to be done for more objects before solid conclusions can be drawn.

Interestingly, the study of outflows on pc-scales using VLBI observations have shown also other interesting features of the HI associated with the outflow. First of

Table 1 Table listing known (and confirmed) broad H I absorption associated with outflows (first part of the list) and broad absorption associated with mergers and binary black holes (second part of the list)

Source name	FWZI $\mathrm{km\,s^{-1}}$	$\dot{M}$ $M_\odot\ \mathrm{yr^{-1}}$	Refs.
IC 5063	750	35	Morganti et al. (1998)
3C 190	600	–	Ishwara-Chandra et al. (2003)
3C 293	1400	8–50	Morganti et al. (2003), Mahony et al. (2013)
3C 305	800	12	Morganti et al. (2005a), Morganti et al. (2005b)
3C 236	1400	47	Morganti et al. (2005a)
4C 12.50	1400	8–21	Morganti et al. (2005a), Morganti et al. (2013)
NGC 1266	400	13[1]	Alatalo et al. (2011), Nyland et al. (2013)
OQ 208	1200	1.2	Morganti et al. (2005a)
4C 52 + 37	674[2]	4	Geréb et al. (2015), Schulz et al. in prep.
3C 459	600	5.5	Morganti et al. (2005a)
4C 31.06	700	–	unpublished (Morganti in prep)
1504 + 377	600	12	Kanekar and Chengalur (2008)
TXS 1200 + 045	600	32	Aditya and Kanekar (2018)
TXS 1245 − 197	1100	18	Aditya and Kanekar (2018)
Mrk 231	1300	8-18	Morganti et al. (2016), Teng et al. (2013)
NGC 3079	600	0.2–2.5	Gallimore et al. (1994), Shafi et al. (2015)
NGC 1068	300[3]	–	Gallimore et al. (1994)
4C37.11	1200	–	Candidate binary BH Maness et al. (2004)
			Morganti et al. (2009b); Rodriguez et al. (2009)
NGC 6420	780	–	Baan et al. (1985); Beswick et al. (2001)

[1] $M_{\mathrm{H\,I+H_2,outflow}}$ from Alatalo et al. (2011)
[2] FW20, from Geréb et al. (2015)
[3] Tentative, see Gallimore et al. (1994)

all, in some objects outflowing gas is also found very close to the active BH (a few tens of pc in projection; 3C 236 and 3C 293, Schulz et al. submitted). Furthermore, the detected outflows appear often to be clumpy with cloud sizes of tens of pc and H I masses of the order of $10^4\ M_\odot$. Such a clumpy medium has been traced in a few cases (e.g. 4C 12.50, 3C 236, 3C 293) and it supports the predictions made by numerical simulations where it is indeed the clumpiness of the medium that enhances the impact of the jet because the jet is meandering through the ISM to find the path of minimum resistance and so creating a cocoon of shocked medium from where the outflow originates.

5.3 Irregular H I structures

Finally, there are situations where H I absorption is not expected to occur, but is nevertheless detected. In such cases, even if H I is not outflowing, it is likely not in a settled configuration and is indicating the presence of extreme conditions.

An example of this is the presence of HI absorption in quasars. Despite the fact that these objects are expected to be pointing close to the line-of-sight and, therefore, not highly obscured, associated absorption has been reported for a few cases (e.g. Pihlström et al. 1999; Ishwara-Chandra et al. 2003) including red-quasars (see, e.g. Carilli et al. 1998b; Yan et al. 2016). In the red quasar 3C190, the detected HI absorption appears to be also broad (with a width of 600 $\mathrm{km\,s^{-1}}$, Ishwara-Chandra et al. 2003 suggesting an ongoing interaction between the jet and the ISM. This is not the only case where the quasars can still be embedded and interacting with a cocoon of gas perhaps originating from the event that has fuelled their central SMBH. This scenario has also been proposed for the radio source PKS 1549-79 (Holt et al. 2006). For this object, an HI profile with only moderate width ($\sim$ 300 $\mathrm{km\,s^{-1}}$) is observed. However, the presence of a fast outflow (with velocities exceeding 1000 $\mathrm{km\,s^{-1}}$) is traced by the ionised gas (Holt et al. 2006) and, more recently, by the molecular gas observed with ALMA (Oosterloo et al. in prep). Interesting is also the case of, although not extremely broad ($<$ 100 $\mathrm{km\,s^{-1}}$), HI absorption blueshifted by about 300 $\mathrm{km\,s^{-1}}$, observed in a blazar object (TXS 1954 + 513, Aditya et al. 2017), likely the result of a recent realignment of the jet axis possibly connected with restarting activity.

A major implication of these results is that the simplest version of the unified schemes may not always hold for young, compact radio sources and confirms that in these objects the jet is interacting with the surrounding medium.

Finally, some other examples of gas structures with extreme kinematics have been found, often with extremely broad ($\geq$ 800 $\mathrm{km\,s^{-1}}$) profiles and detected in objects either undergoing major mergers and, in some cases, showing double nuclei like NGC 6240 (see also Sect. 4.1 for more details), or candidate hosts of binary black holes such as 0402 + 379 (see Morganti et al. 2009b; Rodriguez et al. 2009).

6 Tracing the fuelling of the AGN

Given that HI absorption spectra can sample the immediate environment of a SMBH, the search for signatures of gas fuelling the SMBH has been a central theme since the earliest work on HI absorption. If clouds of cold gas are involved in 'feeding the monster', these clouds could, in principle, be observable as redshifted HI absorption seen against the central radio core. Initial results were encouraging as they seemed to indicate that redshifted HI absorption was more common than absorption at the systemic velocity and even more so than blueshifted absorption (van Gorkom et al. 1989). However, subsequent studies on much larger samples have now shown a clear prevalence of blueshifted (i.e. outflows) over redshifted absorption (i.e. infall). This is particularly evident in samples of young CSS/GPS sources (e.g. Vermeulen et al. 2003a). More recent studies (e.g. Geréb et al. 2015; Maccagni et al. 2017) also show that if the profiles show HI gas deviating from regular rotation, this 'anomalous gas' is mostly seen as blueshifted absorption. The prevalence of blueshifted absorption is likely connected to AGN-driven outflows. Cases of HI absorption with large redshifted velocities do exist, but they are rare (see, e.g. Fig. 5 in Maccagni et al. 2017) and if they are detected, they are deviating less from the systemic velocity than many blueshifted absorptions. The reason for this is still not completely understood. Perhaps HI is not

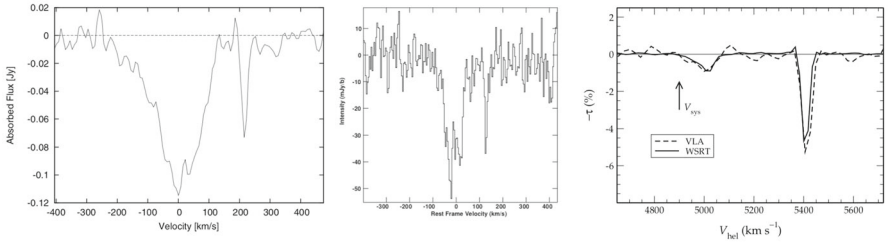

Fig. 18 Examples of radio galaxies where narrows, redshifted H I absorption are seen likely pinpointing the presence of infalling clouds connected with the feeding of the SMBH. Left: integrated absorption spectrum of 4C 31.04 with the velocities shifted to the rest frame of the host galaxy. Middle: H I absorption detected toward the CSO B2352 + 495 after continuum subtraction. The systemic velocity of the system ($V_{Hel} = 71321 \pm 48$ km s^{-1}) is almost at the centroid of the broad absorption feature. Right: H I profile (in optical depth) of the giant radio galaxy NGC 315 obtained from the WSRT (solid line) and the VLA (dashed) data. The two H I absorption systems are clearly visible (see text for details). The systemic velocity is also indicated. Images reproduced with permission from (left) Struve and Conway (2012), copyright by ESO; [middle] from Araya et al. (2010), copyright by AAS; (right) Morganti et al. (2009a), copyright by ESO

involved in feeding the SMBH, but even if it is, it may not be easy to identify redshifted absorption as infalling. Contrary to gas outflows (i.e. blueshifted absorption), for which the velocities involved are determined by the energy input of the AGN and which well exceed the typical gravitational velocity, infall velocities should only slightly exceed the rotational velocities of a regular circumnuclear disk so that the absorption of infalling clouds blends with the absorption of the circumnuclear disk.

At least in some objects, H I is likely connected to feeding the SMBH and infalling clouds of H I have been detected. Often this is indicated by the presence of narrow absorption components redshifted compared to the systemic velocity of the target, some examples are shown in Fig. 18. An example is observed in 4C 31.04 (Conway 1996; Struve and Conway 2012) for which results from VLBA observations (Conway 1999, see Sect. 4.2.2) confirm that its size (5–10 pc) and opacities are similar to those of Galactic High Velocity Clouds which are located in the halo of the Milky Way. Similar results have been found in data of the compact symmetric object B2352 + 495 (Araya et al. 2010) which shows redshifted narrow absorption. The VLBA observations reported by Araya et al. (2010) were not able to localise this component, but the idea of an infalling cloud is the most likely.

However, the situation can be more complex. One interesting case is seen NGC 315. Like in 4C 31.04 and B2352 + 495, a deep, narrow H I absorption line, redshifted by about 500 km s^{-1} from the systemic velocity, was discovered by Dressel et al. (1983) using Arecibo against the inner regions of this giant radio galaxy. The presence of fainter, broader H I absorption closer to the systemic velocity was later revealed by deeper observations (Morganti et al. 2009a). Interestingly, this component is also redshift, albeit only of only $\sim$ 80 km s^{-1} compared to the systemic velocity (see Fig. 18. When traced by the VLBI (i.e. parsec-scales), the two absorption systems have very different structure. The narrow, redshifted absorption smoothly covers most of the central continuum (the core and the inner 10 pc of the jet) and does not show any morphological or kinematic features. This suggests that this component is likely

caused by clouds falling into NGC 315, not necessarily located extremely close to the AGN. Interestingly, the broad component centred on the systemic velocity shows a velocity- as well as a column density gradient (on the scale of only ~ 10 pc) suggesting that the gas has been influenced by the AGN and that it is located physically close to it. Because of these properties and other considerations, it has been suggested that this gas is also involved in fuelling the AGN. If NGC 315 is representative, these data indicate that only observations at high spatial resolution (pc-scales) are able to determine whether gas is close to the AGN and falling into the SMBH.

A similar situation is seen in PKS 2322-123, where identifying the infalling gas could be done in even more detail by the combination of HI and of molecular gas (Tremblay et al. 2016). In this object, both a narrow (110 $\mathrm{km\,s^{-1}}$ FWHM) and a very broad (735 $\mathrm{km\,s^{-1}}$ FWHM) line are seen redshifted ($\sim$ 220 $\pm$ 100 $\mathrm{km\,s^{-1}}$) with respect to the systemic velocity. Thanks to VLBI observations, the location of the components could be determined with the very broad line seen only against the core while the narrow is found about 20 pc from the core (O'Dea et al. 1994; Taylor et al. 1999). These changes on such a small scale suggest that we are looking at gas very close to the nucleus and that the kinematics of the gas can be explained as the result of an atomic torus centred on the nucleus with considerable turbulence and inward streaming motions suggesting infalling gas. This has been nicely confirmed by the ALMA observations of the same object showing absorption due to molecular clouds with similar properties (width and velocities) to the one of the HI (see Tremblay et al. 2016). The combination of the two diagnostics gives strong support to the scenario of inward-moving, clumpy distribution of molecular clouds within a few parsec.

Another extremely interesting case is the very young (~ 100 year) radio galaxy PKS 1718-63 where very narrow absorption lines (both redshifted and blueshifted) were detected. This radio source is only 2 pc in size and the presence of narrow absorption components at different velocities suggests they trace unsettled gas clouds in the inner regions (Véron-Cetty et al. 2000; Maccagni et al. 2014). Extra constraints about their nature come from the detection of redshifted absorption and emission due to molecular clouds in this object (Maccagni et al. 2016, 2018). Thus, also in this object, both atomic and molecular gas show signatures of clouds that can be involved in feeding the recently activated SMBH.

The discovery of such small clouds with unsettled velocities supports the scenario of AGN fuelling known as chaotic cold accretion, now predicted by several numerical simulations (King and Nixon 2015; Gaspari et al. 2013, 2017; Gaspari and Sçdowski 2017). Such models suggest that small clouds of multi-phase gas can condense out of turbulent eddies in the hot gas of the halo of the host galaxy. Angular momentum cancellation occurs via tidal stress and cloud–cloud collisions, resulting in significant inward radial motions of these clouds.

7 Evolution with redshift, effect of UV radiation

Given the importance of gas for the evolution of galaxies, it is not surprising that observing and understanding the changes of the properties of HI absorption with redshift has been a key goal of many absorption studies. Exploring the high-z Universe

using H I absorption has so far been difficult because it is hampered by RFI and by the relatively poor performance of radio telescopes at low frequencies (sensitivity, but also bandpass stability and the presence of standing waves which makes obtaining flat spectral baselines difficult). Published studies have mostly used the GMRT and the GBT. In contrast to the over 150 detections at $z \leq 1$, there are only 7 detections of associated H I 21 cm absorption above this redshift (Ishwara-Chandra et al. 2003; Curran et al. 2013c; Aditya et al. 2017; Aditya and Kanekar 2018) and only two of those are at $z > 2$ (one of which is even a tentative detection; Uson et al. 1991; Aditya et al. 2016).

The few published studies of small samples of objects at high redshift use a variety of selection criteria for the targets. Observed targets include compact radio sources and GPS (Gupta et al. 2006; Aditya and Kanekar 2018), radio quasars and flat spectrum sources (Curran et al. 2008; Aditya et al. 2016), and radio sources selected for their blue magnitude or optical faintness (Curran et al. 2013b, c). The heterogeneity of the samples, and the limited number of objects, makes it particularly difficult to derive strong conclusions about the properties of H I absorption at $z > 1$. Furthermore, the quality of the spectra available is, in most cases, lower than what can be obtained at low redshift. Therefore, a fair comparison with findings at low redshift is still difficult.

Despite these limitations, Curran et al. (2008) were the first to suggest a lower detection rate for sources at $z > 1$ compared to sources below that redshift. This was based on obtaining no detections for all of the ten $z > 3$ sources searched. This study has been followed by other work which, nevertheless, has not been able to fully clarify whether an evolution of the detection rate with redshift is actually present. While a low detection rate was found in the high-z samples by Curran et al. (2013b) and Curran et al. (2013c), the significance of this effect was not fully confirmed by the study of compact flat-spectrum sources—at redshift around 3—selected from the Caltech-Jodrell Bank sample by Aditya et al. (2016). They compare their findings with a lower redshift sample of similarly selected objects reporting marginal evidence for a lower detection rate for the higher redshift sources. The significance (or not) of the trend relies on a tentative detection found at redshift 3.53. In the study of GPS of Aditya et al. (2017), no trend is found when they compare the detection rate with similar studies at low redshift. The final word is likely to come from the new surveys that will be done with the SKA pathfinders (see Sect. 9).

Nevertheless, it is worth discussing whether a possible trend with redshift is due to either limitations of the observations, or due to real physical differences in the high-z objects. One issue is that the high-z samples typically contain objects of higher rest frame luminosities than the sources of the comparison samples at low redshift, in both the radio and the UV wavebands. The population of radio sources studied at high redshift is dominated by very powerful sources ($> 10^{26.5}$ W/Hz) while at low redshift the studied sources are at much lower radio power (see Fig. 4 in Curran and Duchesne 2018). One should also keep in mind that the more powerful sources tend to have relatively faint radio cores, making it difficult to reach low optical depths if the absorption is against the core.

Curran et al. (2008) noted that a high AGN luminosity in either the radio- or the UV band might result in a lower strength of H I absorption. They pointed out that near an AGN with high UV luminosity, the excitation, as well as the ionisation of the hydrogen

gas, may be affected such that it results in a lower incidence of HI absorption. Both redshift evolution and a dependence of local conditions on the AGN UV luminosity were found to be a viable explanations for the observed low occurrence of associated HI absorption in high-z AGN (Curran et al. 2008, 2013b). They also suggested that for high redshifts there is another selection effect, such that the faint optical targets ($B \geq 19$) were in fact UV bright in the source rest-frame, thus ionising/exciting the gas to below the detection limit. They suggest that a critical UV luminosity of $L_{\rm UV} \sim 10^{23}$ W Hz^{-1} exists above which these effects occur. Interestingly, the GPS at redshift 1.275 where recently HI absorption was detected by Aditya and Kanekar (2018) has a high UV luminosity ($> 10^{23}$) as well as an HI outflow with properties similar to found for objects at low redshift.

If the evidence for redshift evolution in the strength of associated HI absorption is confirmed, alternative effects should also be considered as discussed by Aditya et al. (2016). For example, one possibility is that ratio CNM to WNM in high-z objects is typically lower resulting in a higher spin temperature on average. Evidence for an increase of $T_{\rm s}$ with redshift has been obtained by the study of intervening damped Lyman-α systems (e.g. Kanekar et al. 2014 and refs. therein) suggesting a larger fraction of the warm neutral medium. Although the regions of the ISM sampled by damped Lyman-α systems are typically at larger galactic radii and hence not near an AGN, a similar trend could also be present in the environments of high-redshift AGN (Aditya et al. 2016).

8 Connection with other phases of the gas

Obtaining a complete view of the ISM near AGN requires information for all phases of the gas. For this reason, the results obtained from HI absorption are, in most cases, used in combination with other diagnostics, such as ionised gas, and warm and cold molecular gas. There is ample literature on these other gas phases in AGN, far too broad to be covered in this review. Here we describe a few cases where the HI observed in absorption has played a particularly relevant role.

To characterise the properties of the gas in the circumnuclear regions, it of interest to compare the column densities derived from HI absorption with those obtained from absorption of the soft X-ray emission. The X-ray emission from AGN is thought to mostly come from the immediate vicinity of the central BH and resulting from thermal emission from the accretion disc which is reprocessed by the hot plasma in the corona (inverse-Compton scattering). However, in the case of radio galaxies (and especially intrinsically compact CSS/GPS sources), thermal emission from the ISM shocked by the expanding radio lobes, and non-thermal emission from compact lobes produced through inverse-Compton scattering of the local radiation fields, can also play a role.

This X-ray emission can be affected by photoelectric absorption by the foreground consisting of not-fully ionised material in the circumnuclear region. In principle, this absorbing material can be (partly) the same as that producing the HI absorption. However, there are several factors that complicate a comparison between column densities derived from HI absorption with those derived from X-ray observations. While HI absorption provides the column density of neutral hydrogen, X-ray absorption pro-

vides the equivalent total hydrogen column density $N_{\rm H}$ (i.e. atomic, molecular, and ionized hydrogen), of the column of material obscuring the central engine. Therefore, differences in location may play a role, as well as the primary X-ray absorber being dust, molecular or ionised gas, i.e. other phases of the ISM. In addition, the background source which is being absorbed may have a different spatial distribution resulting in differences in the absorption properties, even if the absorber is the same. Moreover, spin temperatures for HI close to an AGN are very uncertain. Also relevant is that the absorption of the X-ray photons is mainly due to elements other than hydrogen so that assumptions on, for example, metallicity have to be made to be able to derive the column density of hydrogen (see, e.g. Wilms et al. 2000).

Studies of a possible a relation between HI column densities derived from HI absorption and hydrogen column densities derived from X-ray observations have brought mixed results. In the case of Seyfert galaxies, Gallimore et al. (1999) find no measurable correlation between HI absorption and absorption columns derived from X-rays (giving a reasonable match only for Mrk 231). For most (eight out of 11) of the sources, the total hydrogen column exceeds the HI column by at least an order of magnitude (see Fig. 14 of Gallimore et al. 1999). Even in Seyfert 2 objects, where obscuration is known to play a major role, the HI absorption column densities are not correlated with the hydrogen column derived from X-ray spectroscopy. This agrees with the result of HI absorption avoiding the very central regions in most Seyferts (see Sect. 4.1).

Similar to what is seen for Seyfert galaxies, for radio galaxies, in particular, GPS and CSS objects, $N_{\rm H}$ is systematically larger than $N_{\rm HI}$ by 1–2 orders of magnitude (e.g. Vink et al. 2006; Tengstrand et al. 2009). On the other hand, trends have been found between $N_{\rm H}$ and $N_{\rm HI}$ suggesting that GPS/CSOs with increasingly large X-ray absorption have increasingly larger probability of being detected in HI absorption observations (Vink et al. 2006; Tengstrand et al. 2009; Ostorero et al. 2010, 2017; Glowacki et al. 2017; Moss et al. 2017).

The detailed analysis of Ostorero et al. (2017) suggests that a correlation exists of the form $N_{\rm H\,I} \sim N_{\rm H}^{b}$, with b ranging between 0.35 and 0.47 depending on the sample used. However, the correlation displays a large scatter which may originate from a scatter of $T_{\rm s}/c_{\rm f}$, the ratio between the spin temperature and the covering factor of the radio continuum needed to estimate $N_{\rm H\,i}$. The observed relation would imply $T_{\rm s}/c_{\rm f}$ to be in the range 12–832 K. This is consistent with the limits on $T_{\rm s}$ derived by Glowacki et al. (2017) and Moss et al. (2017), obtained under the assumption that all of the hydrogen gas producing the X-ray absorption is atomic. They find an upper limit of $T_{\rm spin} \leq 1130 \pm 380$ K assuming a covering factor of 1.

Thus, the gas responsible for the X-ray obscuration and for the HI absorption in compact radio galaxies may be part of the same (settled or unsettled) structure, likely larger than the typical torus, as discussed in Sects. 4.2.2 and 5.1. This result may suggest that the dominant contribution to the X-ray emission of GPS/CSOs does not come from the accretion disc, but from the larger scale jet and lobe components.

Optical spectra can provide a further way to compare HI with ionised gas and with other estimates of the neutral gas. Such comparisons have mostly focussed on characterising gas outflows. Many outflows of ionised gas are known and many of these also have an HI component. In particular, most of the HI outflows found in a

sample of SDSS galaxies seem to have a counter-part of ionised gas (Santoro 2018, Santoro et al. in prep). The converse statement, i.e. outflows detected in ionised gas also showing an H I outflow, is not true. However, this could be, at least partly, due to the limitations of the available data on H I absorption for the optical samples used and deeper data are needed to further investigate this.

Optical spectra can also be used to trace the neutral gas. The most common diagnostic is absorption by the Na D doublet of Na I at 5890 and 5896 Å which can be detected against the optical stellar continuum of the host galaxy. The Na I line is a tracer of cold neutral gas because of its relatively low ionization potential (5.1 eV), quite a bit lower than that of hydrogen (13.6 eV). Thus, depending on the conditions, Na I and H I absorption can trace the same regions of the ISM. However, a direct comparison needs to be done with care. The two tracers are observed in absorption against very different backgrounds, in terms of nature and of extent: the stellar light of the galaxy for Na I and the radio continuum for the H I. A major complication is that the Na I absorption due to the ISM is superposed on Na I absorption occurring in the photospheres of the stars of the stellar background. Moreover, given the relatively low ionisation potential of Na, Na is mostly ionised (i.e. Na II) under many common conditions in the ISM and the conversion from Na I column density to H I column density is not straightforward (see, e.g. Rupke et al. 2002 for a discussion). These complications may explain some of the differences seen in some studies where the two column densities are compared in detail.

Despite all this, consistent results are obtained in a number of cases. In Mrk 231 it is clear that Na I traces the absorption associated with the fast outflow in this galaxy over larger distances from the nucleus compared to the outflow seen in H I absorption against the central radio continuum. Interestingly, the column densities derived from the H I data (ranging from 5 to 15×10^{21} cm^{-2} for $T_s = 1000$ K) are consistent with the column densities derived from the Na I (7.5×10^{21} cm^{-2}; Morganti et al. 2016). This suggests that the Na I and H I absorption may indeed come from the same outflow.

Na I has been used, in particular, for tracing outflows found in ULIRGs (Rupke et al. 2002, 2005; Rupke and Veilleux 2013; Cazzoli et al. 2016; Rupke and Veilleux 2011) and in radio galaxies (Lehnert et al. 2011). The latter studied Na I in radio galaxies selected from FIRST, using SDSS spectra. Interestingly, they find mass- and energy outflow rates of about 10 $M_\odot$ yr^{-1} and few $\times 10^{42}$ erg s^{-1} respectively, consistent with those derived for comparable radio galaxies from H I absorption line observations.

Thanks to new instrumentation, the comparison of the properties of the H I and of the molecular gas in AGN has become much more interesting and relevant. Unsurprisingly, this has been triggered by the very large improvement in observational capabilities provided by ALMA for observations of cold molecular gas, and by NIR instruments for the study of the warm molecular components (e.g. SINFONI and X-Shooter at the VLT). An important aspect is that the boost in sensitivity provided by ALMA is allowing to perform observations of molecular gas in emission at the sub-arcsecond resolution needed to study the structures seen by H I absorption.

Particular attention has been given to molecular gas outflows, after the discovery that not only ionised and atomic neutral hydrogen, but also molecular gas can be found in fast and massive AGN-driven outflows (Feruglio et al. 2010; Cicone et al. 2014). Moreover, the result that in several objects the outflows contain a possibly

even dominant component of molecular gas has given new insights into the physical conditions of the gas close to the AGN and into the physics of the outflows and how they are driven. The fact that molecular outflows appear to be massive and that they have high mass outflow rates, possibly higher than what typically found for the H I outflows (and much higher than the mass outflow rate of the ionised gas) indicates that the molecular gas may represent the most important component for AGN-driven outflows. Clearly, the connection between molecular and atomic outflows has to be understood.

In this context, an important point is that, although the statistics are still limited by small sample sizes, striking similarities have been found between the location and kinematics of the H I and of the molecular gas in outflows in several radio galaxies (see, e.g. Alatalo et al. 2011; Dasyra and Combes 2012; Morganti et al. 2015a, 2016). One of the first examples of this was the CO outflow detected in the radio source 4C12.50 (see Fig. 17). Earlier H I observations (Morganti et al. 2005a) had shown that a fast H I outflow is present in this object which is located at a bright radio hot spot in one of the radio lobes (Morganti et al. 2013). The CO data show absorption over the same velocities as where the H I outflow occurs (Dasyra and Combes 2012).

One of the objects illustrating the similarity between H I and molecular gas kinematics is IC 5063 (see Fig. 19). This is also one of the best examples of the effect of a radio jet entering a clumpy medium, affecting the physical conditions of this medium and producing a fast multiphase outflow (Oosterloo et al. 2017; Mukherjee et al. 2018b). Figure 19 shows the velocity profiles of the cold and the warm molecular gas, of the ionised gas and of the H I. Although the detailed shapes of the profiles differ very much, all phases show the same extent for their blueshifted components, indicating they participate in the same outflow.

The similarity in properties of the atomic and the molecular outflows suggests that both phases are participating in the same processes and that they are driven by a common mechanism. Interestingly, fast outflows of H I and cold molecular gas have been found to be driven by wide-angle winds as well as by radio jets. The discovery of the similarities between the atomic and molecular outflows has triggered large interest in what could be the scenario for accelerating cold gas to the high velocities observed. The model that is currently favoured is that the cold gas forms in situ. After being accelerated and ionised by fast shocks, the outflowing gas is able to cool radiatively on short time scales into clumps of cold molecular material. The H I only represents gas in an intermediate phase, cooling from warm ionised to cold molecular (Zubovas and King 2012; Costa et al. 2015; Richings and Faucher-Giguère 2018). An alternative scenario assumes that pre-existing molecular clouds from the host ISM are entrained in the adiabatically expanding shocked wind and that they are accelerated to the observed velocities without being destroyed (see, e.g. Scannapieco 2017).

An interesting point is that the shared properties of the atomic and molecular outflows, if confirmed for more objects, suggests that the future large H I absorption surveys planned for SKA1 and its precursors, and which are expected to identify many new cases of H I outflows, will also provide many interesting candidates for follow up with ALMA, an instrument not suitable for large, blind surveys. This synergy will greatly help in building up the statistics on the properties of molecular outflows and to help to understand AGN-driven outflows of cold gas in general.

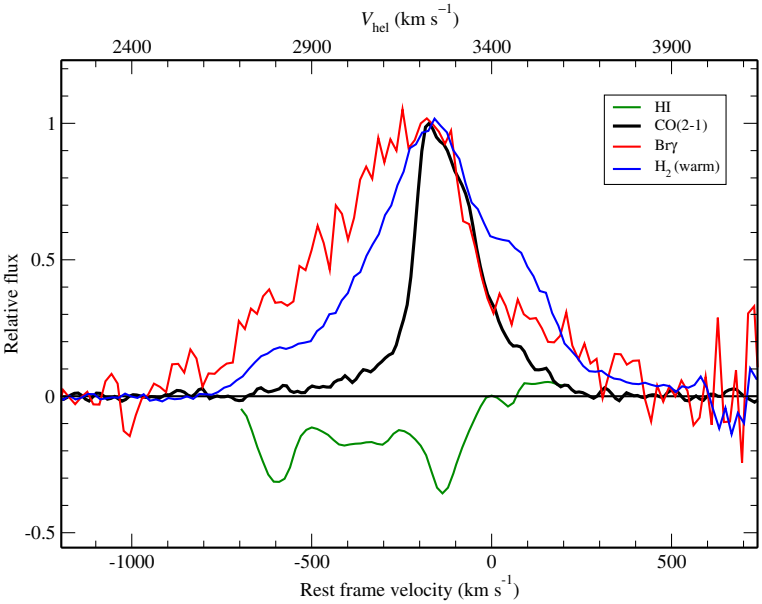

Fig. 19 Velocity profiles of the multiphase outflow in IC 5063. Shown are H_2 1-0 S(1) (blue line) and Brackettγ (red line) velocity profiles for the western lobe of IC 5063 (from Tadhunter et al. 2014), the spatially integrated HI absorption (green line, Morganti et al. 1998) and integrated CO(2-1) spectrum (black line, Morganti et al. 2015b). Although the detailed shapes differ greatly, all phases show the same extent for their blueshifted component indicating they participate in the same outflow. The flux scaling between the different profiles is arbitrary

9 Future perspectives

Significant progress can be expected in the coming years in a number of areas. Much of the work in the next few years will be focussing on exploiting the large survey speed of the SKA pathfinder and precursor telescopes, and later of SKA1 itself. For this purpose, a number of large surveys, which vary in depth and area covered, are being planned (see Table 2; see also Gupta et al. 2018). By utilising the high survey speed, the broad frequency coverage, and the large instantaneous bandwidth of the new telescopes, these surveys will allow to create large, new samples of objects out to high redshift, which will be used to explore new territory (see Morganti et al. 2015a). The expected number of detections will increase the number of known associated HI absorptions (currently about 150) by almost two orders of magnitude with the majority of the detections in a redshift range that is poorly sampled currently (Table 2). This will make it much easier to compare the absorption properties of various classes of objects. A very important difference is that the planned surveys will carry out blind searches for HI absorption in contrast to the targeted surveys done so far. This will allow to probe the HI and its properties, and the evolution thereof, in radio sources in a much more systematic and unbiased way.

A peek of things to come is shown in Fig. 20 which shows a spectrum taken from commissioning observations done with the ASKAP test array BETA (see also Allison

Table 2 Summary of upcoming large H I 21 cm absorption line surveys (see also Morganti et al. (2015a); Gupta et al. (2018)

Survey	Redshift range	Noise over 5 km s^{-1} [mJy beam^{-1}]	Sky coverage [deg^2]	Number of detections	Detection limit [mJy]
Apertif-SHARP	0–0.26	1.3	4000	400	30
ASKAP-FLASH	0.4–1.0	3.8	25 000	5500	90
ASKAP-Wallaby	0–0.26	1.6	30 000	2300	40
MeerKAT-MALS (L-band)	0–0.57	0.5	1300	450	15
MeerKAT-MALS (UHF-band)	0.40–1.44	0.5–0.7	2000	1500	15

SHARP and WALLABY are commensal H I emission and absorption surveys, primarily investigating associated absorption. FLASH is a blind survey of the southern hemisphere to detect H I absorption in intervening and associated systems at intermediate redshifts. The MALS project is targeted survey focussing on relatively bright, high redshift background sources to search the line of sight for intervening absorption (Gupta et al. 2018). However, with the more than 1×1 deg^2 field of view of MeerKAT, a substantial volume for each pointing is blindly, and commensally, probed both for associated and intervening absorbers. The expected number of detections has been estimated using the redshift distribution of radio sources from the S-cubed simulations (Wilman et al. 2008) and assuming a detection rate for associated absorption of 25%

et al. 2015, 2017). The spectrum covers the redshift range $0 < z < 1$ with a velocity resolution of only a few km s^{-1}. For each continuum source in the survey area, one will be able to obtain such a spectrum covering such a large range in redshift. This means that the presence of H I can be recovered also for galaxies for which the redshift is not known a priori. Thus, the planned surveys will provide a 'blind view' of a very large volume of the Universe. Particularly exciting is the possibility of having a first proper census at higher redshifts thanks to the higher sensitivity at lower frequencies and the low RFI levels at the locations of the new radio telescopes. In the slightly more distant future, the higher sensitivity and the even larger frequency coverage of SKA1 will make sure that the above planned surveys can be expanded to fainter and to more distant sources. The higher sensitivity of MeerKat and of SKA1 compared to available radio telescopes also means that fainter H I absorption can be detected. This is particularly relevant for studying fast H I outflows, the study of which is now limited to relatively bright sources, given the low opacities involved.

Figure 21 (taken from Maccagni et al. 2017) illustrates another aspect of the upcoming surveys, namely their complementarity in terms of depth and redshift coverage (interestingly, this came about largely by coincidence…). The figure indicates the expected number of detections of the various surveys, as function of source luminosity and redshift. The parts of parameter space over which the different surveys will detect sources match very nicely and in particular sources with a luminosity in the range 10^{26}–10^{27} W Hz^{-1} can be studied over a large redshift range. This will allow to construct well-selected samples of objects up to $z \sim 1.5$ and perform studies of the evolution of gas in AGN probing optical depths of a few % and H I column densities of 10^{20}–10^{21} cm^{-2}.

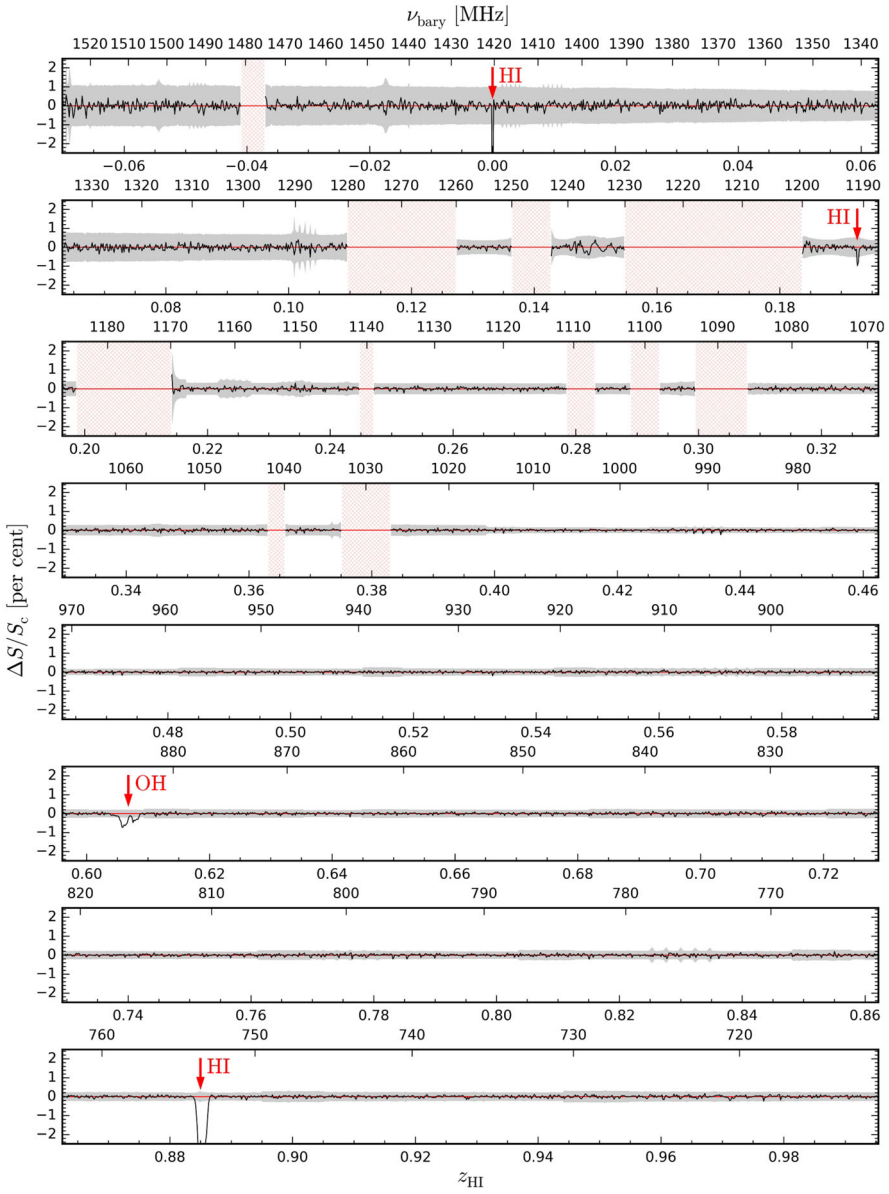

Fig. 20 A spectrum obtained with the ASKAP test array BETA towards the gravitational lensed quasar PKS B1830-211. This figure illustrates the possibilities of the new generation of receivers. In the case shown here, the receiver can cover—with just three observations—a redshift range going from 0 to 1 and detect any HI in this range located along the line of sight. The hatched regions mask data that were significantly contaminated by aviation and satellite-generated RFI. The red arrows indicate the positions of previously reported HI and OH lines. Images reproduced with permission from Allison et al. (2017), copyright by the authors

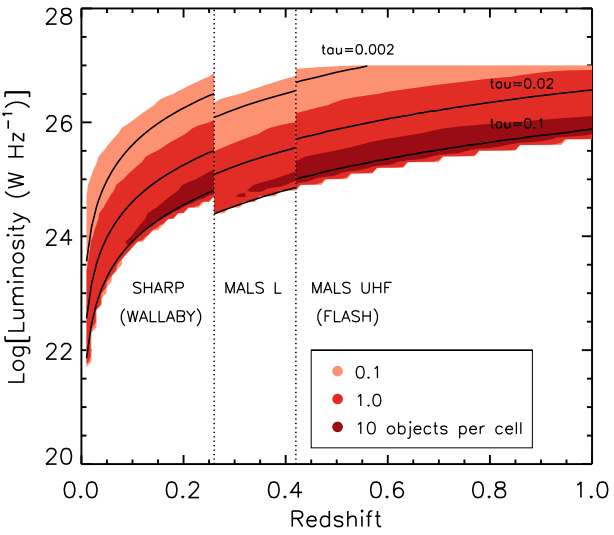

Fig. 21 Coverage of the luminosity-redshift plane by upcoming absorption surveys. The parameter space is divided into cells of $dz = 0.01$ and $dL = 0.1$, and the colour coding indicates 0.1 (light), 1 (medium), and 10 (dark shading) objects per cell. As expected, the majority of objects lie close to the flux limits of the surveys. At $z \leq 0.26$, SHARP in the northern hemisphere and WALLABY in the south cover very similar parameter space. The full MALS L-band survey covers $0 < z < 0.58$, but is the only survey probing intermediate redshifts, $0.26 < z < 0.42$. MALS UHF targets intermediate redshifts, $0.42 < z < 1.44$. A similar redshift range is covered by FLASH, but with brighter flux limits. For clarity, we show the coverage of the plane out to $z = 1$, even though MALS UHF extends to $z = 1.44$ with the same behaviour. The black lines denote the minimum optical depth visible for sources of a given flux with the channel noise values. Image reproduced with permission from Maccagni et al. (2017), copyright by ESO

Observations to higher redshifts (up to $\sim$ 3) can be done, at present, only with the GMRT and with single dish telescopes, like the GBT. However, low frequency telescopes like LOFAR (van Haarlem 2013), MWA (Tingay et al. 2013) and ultimately SKA-Low are now opening the challenging but exciting possibility to explore HI in even higher redshift objects (i.e. $z \sim$ 5–10). The fact that some of the very high-z radio sources have been detected in molecular gas (see, e.g. Klamer et al. 2005; Emonts et al. 2018), makes such absorption studies extremely relevant.

For these blind surveys, automated detection techniques have already been developed (Allison et al. 2012, 2014; Koribalski 2012), along with techniques for stacking absorption spectra (Geréb et al. 2014) and profile characterisation (Geréb et al. 2015) of large samples. The pathfinder and precursor surveys will allow us to expand the use of stacking techniques and derive general properties of groups of objects such as young vs old vs restarted radio sources, compact vs extended objects, and exploring trends with redshift, optical properties etc..

Since most of the planned surveys will be done on the southern sky, they will provide interesting targets for follow-up with the excellent optical and mm facilities which are, or soon will be, available in the southern hemisphere. In particular, the blind searches for HI outflows will provide targets for observation with ALMA to investigate the

molecular counterpart of the outflows. Future large-area optical spectroscopic surveys planned in both hemispheres will also be an important complement to the HI data.

10 Conclusions

In this review we have summarised the main results based on HI 21 cm absorption observations obtained in the last two decades about the cold ISM in the central regions of radio loud galaxies and about the interplay between this gas and the AGN. Given the specific nature of HI absorption observations, they make it possible to study the cold gas in the environment of AGN at parsec scales also at higher redshift and therefore can probe a completely different parameter space than observations of HI emission. Significant progress has been made in a number of important areas, in part due to technical improvements of radio telescopes which have allowed to obtain data over larger bandwidths and with higher spectral dynamic range. The main results can be summarised as follows:

- Observations of various samples of various types of radio sources have shown that AGN are surrounded by a regularly rotating gas disk which contains a detectable fraction of HI, as expected from theoretical models. In low-power objects, these disks are thin and are typically a few hundred parsec in size. In more powerful objects, they extend to smaller radii and are thicker. In Seyfert galaxies, these disks connect to the larger scale galactic disks. Due to obscuration effects, these disks play a role in how the central AGN is detected in other wavebands. In radio galaxies, the presence of circumnuclear absorbing structures containing HI is by now well established and the kinematics of these structures has been traced by pc-resolution VLBI observations. Some groups of objects, and in particular young and recently restarted radio galaxies, appear to have a particularly high detection rate of HI. This is interesting in connection with the evolution of these AGN and their impact on the surrounding ISM.
- An important discovery has been the occurrence of fast (> 1000 km s^{-1}) HI outflows in about 5% of radio sources. They occur, in particular, in young radio sources. High-spatial resolution observations have shown that most of these outflows are driven by the radio jet coming from the central AGN, but they can also be driven by wide-angle nuclear winds. These outflows of atomic hydrogen have a counterpart of molecular outflows. The preferred model is that the cold gas is the result of fast cooling of the gas after it has been shocked and accelerated by a passing jet, or by a cocoon of overpressured gas inflated by the jet. The observed mass outflow rates of the cold gas in these outflows are much larger than those of the ionised outflows. This has provided a completely new way to look at the gas under the influence of the energy released by an active BH which is important input on the role of AGN feedback in models of galaxy evolution.
- It has been more difficult than anticipated to detect evidence for HI playing a role in fuelling the central SMBH. The original consensus that redshifted absorption components, which would indicate accretion onto the SMBH, occur more often than blueshifted components has made place for the reverse namely that blueshifted

absorption is more common and also extends to more extreme velocities. It may not be easy to identify redshifted absorption as infalling given that infall velocities should be similar to the rotational velocities of a regular circumnuclear disk and the absorption of infalling clouds may blend with the absorption of the circumnuclear disk. Nevertheless, a small number of high-resolution observations have shown evidence for fuelling. These observations also suggest that infalling H I can only be identified as such in high-resolution data

The results summarised above show the exciting progress of the last two decades in the field of associated H I absorption and the many significant contributions which have been made for better understanding the cold ISM near AGN and the role it plays in the evolution of AGN and of their host galaxies. It is very likely that a review on H I absorption that will be written in two decades from now will contain even more exciting and important results. The new blind large-area surveys which will be done with several new radio facilities in the near future will have a major impact on H I absorption studies. The number of detections of associated H I absorption will increase by a very large factor ($\gg 10$) and the data will extend to fainter source populations and fainter absorption features. Very important is the fact that the new surveys are blind surveys. This will to a large extent remove the effects of many selection biases which now plague most studies and which makes drawing firm conclusions sometimes difficult. Perhaps the most exciting prospect is offered by the improved sensitivity at higher redshift. This will provide a major step forward for studying the evolution with redshift of the gas in AGN, something which has been very difficult to up to now.

Acknowledgements We would like to thank James Allison and Elaine Sadler for their insightful input. RM gratefully acknowledges support from the European Research Council under the European Union's Seventh Framework Programme (FP/2007-2013) /ERC Advanced Grant RADIOLIFE-320745.

References

Aditya JNHS, Kanekar N, Kurapati S (2016) A giant metrewave radio telescope search for associated H I 21 cm absorption in high-redshift flat-spectrum sources. Mon Not R Astron Soc 455:4000–4012

Aditya JNHS, Kanekar N, Prochaska JX, Day B, Lynam P, Cruz J (2017) Giant metrewave radio telescope detection of associated H I 21-cm absorption at $z = 1.2230$ towards TXS 1954+513. Mon Not R Astron Soc 465:5011–5015

Aditya JNHS, Kanekar N (2018) A giant metrewave radio telescope search for associated H I 21 cm absorption in GHz-peaked-spectrum sources. Mon Not R Astron Soc 473:59–67

Alatalo K et al (2011) Discovery of an active galactic nucleus driven molecular outflow in the local early-type galaxy NGC 1266. Astrophys J 735:88

Allison JR, Sadler EM, Whiting MT (2012) Application of a Bayesian method to absorption spectral-line finding in simulated data. Publ Astron Soc Aust 29:221–228

Allison JR, Sadler EM, Meekin AM (2014) A search for H I absorption in nearby radio galaxies using HIPASS. Mon Not R Astron Soc 440:696–718

Allison JR et al (2015) Discovery of H I gas in a young radio galaxy at $z = 0.44$ using the Australian square kilometre array pathfinder. Mon Not R Astron Soc 453:1249–1267

Allison JR et al (2017) Illuminating the past 8 billion years of cold gas towards two gravitationally lensed quasars. Mon Not R Astron Soc 465:4450–4467
Araya ED, Rodríguez C, Pihlström Y, Taylor GB, Tremblay S, Vermeulen RC (2010) VLBA observations of H I in the archetype compact symmetric object B2352+495. Astron J 139:17–26
Argo MK, van Bemmel IM, Connolly SD, Beswick RJ (2015) A new period of activity in the core of NGC 660. Mon Not R Astron Soc 452:1081–1088
Baan WA, Haschick AD, Buckley D, Schmelz JT (1985) Hydroxyl absorption in NGC 520, NGC 2623, and NGC 6240. Astrophys J 293:394–399
Baan WA, Rhoads J, Haschick AD (1992) OH and H I absorption at the nucleus of NGC 660. Astrophys J 401:508–515
Baan WA, Hagiwara Y, Hofner P (2007) H I and OH Absorption toward NGC 6240. Astrophys J 661:173–184
Bahcall JN, Ekers RD (1969) On the possibility of detecting redshifted 21-cm absorption lines in the spectra of quasi-stellar sources. Astrophys J 157:1055
Beswick RJ, Pedlar A, Mundell CG, Gallimore JF (2001) A MERLIN neutral hydrogen absorption study of the luminous infrared merger NGC 6240. Mon Not R Astron Soc 325:151–158
Beswick RJ, Peck AB, Taylor GB, Giovannini G (2004) Mon Not R Astron Soc 352:49
Bourke et al (eds) (2014) Advancing astrophysics with the square kilometre array, 9–13 June, 2014, Giardini Naxos, Italy. In: Proceedings of science, vol AASKA14. http://pos.sissa.it/cgi-bin/reader/conf.cgi?confid=215
Cappellari M et al (2011) The ATLAS^{3D} project - I. A volume-limited sample of 260 nearby early-type galaxies: science goals and selection criteria. Mon Not R Astron Soc 413:813–836
Carilli CL, Wrobel JM, Ulvestad JS (1998a) A subkiloparsec disk in Markarian 231. Astron J 115:928–937
Carilli CL, Menten KM, Reid MJ, Rupen MP, Yun MS (1998b) Redshifted neutral hydrogen 21 centimeter absorption toward red quasars. Astrophys J 494:175–182
Cazzoli S, Arribas S, Maiolino R, Colina L (2016) Neutral gas outflows in nearby [U]LIRGs via optical NaD feature. Astron Astrophys 590:A125
Chandola Y, Saikia DJ, Gupta N (2010) H I gas in the rejuvenated radio galaxy 4C29.30. Mon Not R Astron Soc 403:269–273
Chandola Y, Sirothia SK, Saikia DJ (2011) H I absorption towards nearby compact radio sources. Mon Not R Astron Soc 418:1787–1795
Chandola Y, Sirothia SK, Saikia DJ, Gupta N (2012) Associated H I absorption towards the core of the radio galaxy 3C 321. Bull Astron Soc India 40:139–150
Chandola Y, Gupta N, Saikia DJ (2013) Associated 21-cm absorption towards the cores of radio galaxies. Mon Not R Astron Soc 429:2380–2391
Chandola Y, Saikia DJ (2017) H I absorption towards low-luminosity radio-loud active galactic nuclei of different accretion modes and WISE colours. Mon Not R Astron Soc 465:997
Chiaberge M, Capetti A, Celotti A (1999) The HST view of FR I radio galaxies: evidence for non-thermal nuclear sources. Astron Astrophys 349:77–87
Christiansen WN, Hindman JV (1952) 21 cm. line radiation from galactic hydrogen. Observ 72:149–151
Cicone C, Maiolino R, Sturm E et al (2014) Massive molecular outflows and evidence for AGN feedback from CO observations. Astron Astrophys 562:A21
Combes F et al (2013) ALMA observations of feeding and feedback in nearby Seyfert galaxies: an AGN-driven outflow in NGC 1433. Astron Astrophys 558:A124
Conway JE, Blanco PR (1995) H I Absorption Toward the Nucleus of the Powerful Radio Galaxy Cygnus A: Evidence for an Atomic Obscuring Torus? Astrophys J 449:L131
Conway JE (1996) A circumnuclear H I disk in the compact symmetric object 4C31.04? In: Ekers R, Fanti C, Padrielli L (eds) Extragalactic radio sources, vol 175. Kluwer, International Astronomical Union, pp 92–94
Conway JE (1999) VLBI spectral absorption in AGN. New Astron Rev 43:509–513
Conway JE, Schilizzi RT (2000) H I absorption in 3C236. EVN Symposium 2000. In: Proceedings of the 5th European VLBI network symposium 123
Costa T, Sijacki D, Haehnelt MG (2015) Fast cold gas in hot AGN outflows. Mon Not R Astron Soc 448:L30–L34
Crane P, van der Hulst J, Haschick A (1982) Detection of a broad H I absorption feature at 5300-KM/SEC associated with NGC1275 / 3C84. Extragalactic Radio Sour 97:307

Curran SJ, Whiting MT, Wiklind T, Webb JK, Murphy MT, Purcell CR (2008) A survey for redshifted molecular and atomic absorption lines - II. Associated H I, OH and millimetre lines in the $z \gtrsim 3$ Parkes quarter-Jansky flat-spectrum sample. Mon Not R Astron Soc 391:765–784
Curran SJ, Whiting MT (2010) H I 21 cm absorption and unified schemes of active galactic nuclei. Astrophys J 712:303–317
Curran SJ, Allison JR, Glowacki M, Whiting MT, Sadler EM (2013a) On the H I column density-radio source size anticorrelation in compact radio sources. Mon Not R Astron Soc 431:3408–3413
Curran SJ, Whiting MT, Sadler EM, Bignell C (2013b) A survey for the missing hydrogen in high-redshift radio sources. Mon Not R Astron Soc 428:2053–2063
Curran SJ, Whiting MT, Tanna A, Sadler EM, Pracy MB, Athreya R (2013c) A survey for H I in the distant Universe: the detection of associated 21-cm absorption at $z = 1.28$. Mon Not R Astron Soc 429:3402–3410
Curran SJ, Duchesne SW (2018) The mid-infrared properties and gas content of active galaxies over large look-back times. Mon Not R Astron Soc MNRAS 476:3580–3590
Dasyra KM, Combes F (2012) Cold and warm molecular gas in the outflow of 4C 12.50. Astron Astrophys 541:L7
De Young DS, Roberts MS, Saslaw WC (1973) Detection of 21-centimeter hydrogen absorption in the high-velocity component of the radio galaxy perseus A. Astrophys J 185:809–816
Dickey JM (1982) VLA observations of H I absorption in the nuclei of Seyfert and active galaxies. Astrophys J 263:87–93
Dressel LL, Davis MM, Bania TM (1983) NGC 315: high-velocity H I in an active elliptical galaxy. Astrophys J 266:L97–L101
Edge AC (2001) The detection of molecular gas in the central galaxies of cooling flow clusters. Mon Not R Astron Soc 328:762–782
Emonts BHC, Morganti R, Struve C, Oosterloo TA, van Moorsel G et al (2010) Large-scale H I in nearby radio galaxies - II. The nature of classical low-power radio sources. Mon Not R Astron Soc 406:987–1006
Emonts BHC et al (2018) Giant galaxy growing from recycled gas: ALMA maps the circumgalactic molecular medium of the Spiderweb in [C I]. Mon Not R Astron Soc 477:L60–L65
Espada D et al (2010) Disentangling the circumnuclear environs of Centaurus A. II. On the nature of the broad absorption line. Astrophys J 720:666–678
Ewen HI, Purcell EM (1951) Observation of a line in the galactic radio spectrum: radiation from galactic hydrogen at 1,420 Mc./sec. Nature 168:356
Fernández X et al (2016) Highest redshift image of neutral hydrogen in emission: a CHILES detection of a starbursting galaxy at $z = 0.376$. Astrophys J 824:L1
Feruglio C, Maiolino R, Piconcelli E, Menci N, Aussel H, Lamastra A, Fiore F (2010) Quasar feedback revealed by giant molecular outflows. Astron Astrophy 518:L155
Field GB (1959) The spin temperature of intergalactic neutral hydrogen. Astrophys J 129:536
Fragile PC, Murray SD, Anninos P, van Breugel W (2004) Radiative shock-induced collapse of intergalactic clouds. ApJ 604:74
Gallimore JF, Baum SA, O'Dea CP, Brinks E, Pedlar A (1994) Neutral hydrogen absorption in NGC 1068 and NGC 3079. Astrophys J 422:L13–L16
Gallimore JF, Baum SA, O'Dea CP, Pedlar A, Brinks E (1999) Neutral hydrogen (21 centimeter) absorption in seyfert galaxies: evidence for free-free absorption and Subkiloparsec gaseous disks. Astrophys J 524:684–706
Gaspari M, Ruszkowski M, Oh SP (2013) Chaotic cold accretion on to black holes. Mon Not R Astron Soc 432:3401–3422
Gaspari M, Temi P, Brighenti F (2017) Raining on black holes and massive galaxies: the top-down multiphase condensation model. Mon Not R Astron Soc 466:677–704
Gaspari M, Sçdowski A (2017) Unifying the micro and macro properties of AGN feeding and feedback. Astrophys J 837:149
Geréb K (2014) The role of neutral hydrogen in the life of galaxies and AGN: a spectral stacking analysis, PhD Thesis, University of Groningen. https://www.rug.nl/research/portal/en/publications/the-role-of-neutral-hydrogen-in-the-life-of-galaxies-and-agn(851c71b8-337a-438b-9b8c-fe010f3cdae1).html
Geréb K, Morganti R, Oosterloo TA (2014) Probing the gas content of radio galaxies through H I absorption stacking. Astron Astrophys 569:A35

Geréb K, Maccagni FM, Morganti R, Oosterloo TA (2015) The H I absorption "Zoo". Astron Astrophys 575:A44
Giovanelli R, Haynes MP (2015) Extragalactic H I surveys. Astron Astrophys Rev 24:1
Giovannini G, Feretti L, Gregorini L, Parma P (1988) Radio nuclei in elliptical galaxies. Astron Astrophys 199:73–84
Glowacki M, Allison JR, Sadler EM, Moss VA, Curran SJ, Musaeva A, Deng C, Parry R, Sligo MC (2017) H I absorption in nearby compact radio galaxies. Mon Not R Astron Soc 467:2766–2786
Gupta N, Srianand R, Saikia DJ (2005) Outflowing material in the compact steep-spectrum source quasar 3C 48: evidence of jet-cloud interaction? Mon Not R Astron Soc 361:451–459
Gupta N, Salter CJ, Saikia DJ, Ghosh T, Jeyakumar S (2006) Probing radio source environments via H I and OH absorption. Mon Not R Astron 373:972–992
Gupta N, Saikia DJ (2006) Unification scheme and the distribution of neutral gas in compact radio sources. Mon Not R Astron Soc 370:738–742
Gupta Y et al (2017) The upgraded GMRT: opening new windows on the radio Universe. Curr Sci 113:707
Gupta N et al (2018) The MeerKAT absorption line survey (MALS). In: Taylor R et al (eds) MeerKAT science: on the pathway to the SKA, 25–27 May, 2016, Stellenbosch, South Africa, Proceedings of Science vol. MeerKAT2016. https://pos.sissa.it/277/014/
van Haarlem MP et al (2013) LOFAR: the LOw-Frequency ARray. Astron Astrophys 556:A2
Heckman TM, Balick B, van Breugel WJW, Miley GK (1983) Observations of neutral hydrogen in radio-loud and interacting galaxies. Astron J 88:583–597
Heckman TM (2002) Galactic Superwinds Circa 2001. Extragalactic Gas Low Redshift 254:292
Heckman TM, Best PN (2014) The coevolution of galaxies and supermassive black holes: insights from surveys of the contemporary universe. Annu Rev Astron Astrophys 52:589–660
Hogan MT (2014) The radio properties of brightest cluster galaxies. PhD Thesis, University of Durham. http://etheses.dur.ac.uk/11008/
Holt J, Tadhunter C, Morganti R, Bellamy M, González Delgado RM, Tzioumis A, Inskip KJ (2006) The co-evolution of the obscured quasar PKS 1549–79 and its host galaxy: evidence for a high accretion rate and warm outflow. Mon Not R Astron Soc 370:1633–1650
Ishwara-Chandra CH, Dwarakanath KS, Anantharamaiah KR (2003) GMRT detection of H I 21 cm associated absorption towards the $z = 1.2$ Red Quasar 3C 190. J Astrophys Astron 24:37
Jaffe W (1990) 21-cm H I absorption in NGC 1275. Astron Astrophys 240:254–258
Kanekar N, Briggs FH (2004) 21-cm absorption studies with the Square Kilometer Array. New Astron Rev 48:1259–1270
Kanekar N, Chengalur JN (2008) Outflowing atomic and molecular gas at $z \sim 0.67$ towards 1504 + 377. Mon Not R Astron Soc 384:L6–L10
Kanekar N, Braun R, Roy N (2011) An H I column density threshold for cold gas formation in the galaxy. Astrophys J 737:L33
Kanekar N et al (2014) The spin temperature of high-redshift damped Lyman α systems. Mon Not R Astron Soc 438:2131–2166
King A, Nixon C (2015) AGN flickering and chaotic accretion. Mon Not R Astron Soc 453:L46–L47
Klamer IJ, Ekers RD, Sadler EM, Weiss A, Hunstead RW, De Breuck C (2005) CO (1–0) and CO (5–4) observations of the most distant known radio galaxy at $z = 5.2$. Astrophys J 621:L1–L4
Koribalski BS (2012) Source Finding and Visualisation. Publ Astron Soc Aust 29:213–213
Krolik JH (1988) The origin of broad emission line clouds in active galactic nuclei. Astrophys J 325:148–152
Labiano A, Vermeulen RC, Barthel PD, O'Dea CP, Gallimore JF, Baum S, de Vries W (2006) H I absorption in 3C 49 and 3C 268.3. Probing the environment of compact steep spectrum and GHz peaked spectrum sources. Astron Astrophys 447:481–487
Lehnert MD, Tasse C, Nesvadba NPH, Best PN, van Driel W (2011) The Na D profiles of nearby low-power radio sources: jets powering outflows. Astron Astrophys 532:L3
Lynds R (1970) Improved photographs of the NGC 1275 phenomenon. Astrophys J 159:L151–L154
Liszt H (2001) Astron Astrophys 371:865
Maccagni FM, Morganti R, Oosterloo TA, Mahony EK (2014) What triggers a radio AGN?. The intriguing case of PKS B1718–649. Astron Astrophys 571:A67
Maccagni FM, Santoro F, Morganti R et al (2016) The warm molecular hydrogen of PKS B1718–649. Feeding a newly born radio AGN. Astron Astrophys 588:A46

Maccagni FM, Morganti R, Oosterloo TA, Geréb K, Maddox N (2017) Kinematics and physical conditions of H I in nearby radio sources. The last survey of the old Westerbork synthesis radio telescope. Astron Astrophys 604:A43
Maccagni FM, Morganti R, Oosterloo TA, Oonk JBR, Emonts BHC (2018) ALMA observations of AGN fuelling: the case of PKS B1718–649. Astron Astrophys 614:A42
Mahony EK, Morganti R, Emonts BHC, Oosterloo TA, Tadhunter C (2013) The location and impact of jet-driven outflows of cold gas: the case of 3C 293. Mon Not R Astron Soc 435:L58–L62
Maloney PR, Hollenbach DJ, Tielens AGGM (1996) X-ray-irradiated molecular gas. I. Physical processes and general results. Astrophys J 466:561
Maness HL, Taylor GB, Zavala RT, Peck AB, Pollack LK (2004) Breaking all the rules: the compact symmetric object 0402+379. ApJ 602:123
Mellema G, Kurk JD, Röttgering HJA (2002) Evolution of clouds in radio galaxy cocoons. A&A 395:L13
Mirabel IF (1982) Neutral hydrogen in bright galaxies with strong radio sources. Astrophys J 260:75–80
Mirabel IF (1989) Atomic hydrogen in the powerful radio-infrared galaxies 4C 12.50 and 3C 433. Astrophys J 340:L13–L16
Momjian E, Romney JD, Troland TH (2002) Global VLBI observations of the high-velocity H I absorption toward NGC 1275. Astrophys J 566:195–201
Morganti R, Oosterloo TA, Reynolds JE, Tadhunter CN, Migenes V (1997) A study of cores in a complete sample of radio sources. Mon Not R Astron Soc 284:541–551
Morganti R, Oosterloo T, Tsvetanov Z (1998) A radio study of the seyfert galaxy IC 5063: evidence for fast gas outflow. Astron J 115:915–927
Morganti R, Oosterloo TA, Tadhunter CN, van Moorsel G, Killeen N, Wills KA (2001) H I absorption in radio galaxies: effect of orientation or interstellar medium? Mon Not R Astron Soc 323:331–342
Morganti R, Oosterloo TA, Emonts BHC, van der Hulst JM, Tadhunter CN (2003) Fast outflow of neutral hydrogen in the radio galaxy 3C 293. Astrophys J 593:L69–L72
Morganti R, Greenhill LJ, Peck AB, Jones DL, Henkel C (2004) Disks, tori, and cocoons: emission and absorption diagnostics of AGN environments. New Astron Rev 48:1195–1209
Morganti R, Tadhunter CN, Oosterloo TA (2005a) Fast neutral outflows in powerful radio galaxies: a major source of feedback in massive galaxies. Astron Astrophys 444:L9–L13
Morganti R, Oosterloo TA, Tadhunter CN, van Moorsel G, Emonts B (2005b) The location of the broad H I absorption in 3C 305: clear evidence for a jet-accelerated neutral outflow. Astron Astrophys 439:521–526
Morganti R, de Zeeuw PT, Oosterloo TA, McDermid RM, Krajnović D, Cappellari M, Kenn F, Weijmans A, Sarzi M (2006) Neutral hydrogen in nearby elliptical and lenticular galaxies: the continuing formation of early-type galaxies. Mon Not R Astron Soc 371:157–169
Morganti R, Oosterloo T, Struve C, Saripalli L (2008) A circumnuclear disk of atomic hydrogen in Centaurus A. Astron Astrophys 485:L5–L8
Morganti R, Peck AB, Oosterloo TA, van Moorsel G, Capetti A, Fanti R, Parma P, de Ruiter HR (2009) Is cold gas fuelling the radio galaxy NGC 315? Astron Astrophys 505:559–567
Morganti R, Emonts B, Oosterloo T (2009) Broad H I absorption in the candidate binary black hole 4C37.11 (B2 0402+379). Astron Astrophys 496:L9–L12
Morganti R, Holt J, Tadhunter C, Ramos Almeida C, Dicken D, Inskip K, Oosterloo T, Tzioumis T (2011) PKS 1814–637: a powerful radio-loud AGN in a disk galaxy. Astron Astrophys 535:A97
Morganti R, Fogasy J, Paragi Z, Oosterloo T, Orienti M (2013) Radio Jets clearing the way through a galaxy: watching feedback in action. Science 341:1082–1085
Morganti R, Sadler EM, Curran S (2015a) Cool Outflows and H I absorbers with SKA. Adv Astrophys Square Kilometre Array (AASKA14) 134
Morganti R, Oosterloo T, Oonk JBR, Frieswijk W, Tadhunter C (2015b) The fast molecular outflow in the Seyfert galaxy IC 5063 as seen by ALMA. Astron Astrophys 580:A1
Morganti R, Veilleux S, Oosterloo T, Teng SH, Rupke D (2016) Another piece of the puzzle: The fast H I outflow in Mrk 231. Astron Astrophys 593:A30
Morganti R (2017) The many routes to AGN feedback. Front Astron Space Sci 4:42
Moss VA et al (2017) Connecting X-ray absorption and 21 cm neutral hydrogen absorption in obscured radio AGN. Mon Not R Astron Soc 471:2952–2973
Mukherjee D, Bicknell GV, Sutherland R, Wagner A (2016) Relativistic jet feedback in high-redshift galaxies - I Dynamics. Mon Not R Astron 461:967–983

Mukherjee D, Wagner AY, Bicknell GV, Morganti R, Oosterloo T, Nesvadba N, Sutherland RS (2018) The jet-ISM interactions in IC 5063. Mon Not R Astron Soc 476:80–95
Mukherjee D, Bicknell GV, Wagner AY, Sutherland RS, Silk J (2018) Relativistic jet feedback III: feedback on gas disks. arXiv:1803.08305
Muller CA, Oort JH (1951) Observation of a line in the galactic radio spectrum: the interstellar hydrogen line at 1,420 Mc./sec., and an estimate of galactic rotation. Nature 168:357–358
Mundell CG, Pedlar A, Baum SA, O'Dea CP, Gallimore JF, Brinks E (1995) MERLIN observations of neutral hydrogen absorption in the Seyfert nucleus of NGC 4151. Mon Not R Astron Soc 272:355–362
Mundell CG, Ferruit P, Pedlar A (2001) Nuclear gasdynamics in Arp 220: Subkiloparsec-scale atomic hydrogen disks. Astrophys J 560:168–177
Nyland K et al (2017) Star formation in nearby early-type galaxies: the radio continuum perspective. Mon Not R Astron Soc 464:1029–1064
Nyland K, Alatalo K, Wrobel JM, Young LM, Morganti R, Davis TA, de Zeeuw PT, Deustua S, Bureau M (2013) Detection of a high brightness temperature radio core in the active-galactic-nucleus-driven molecular outflow candidate NGC 1266. Astrophys J 779:173
O'Dea CP, Baum SA, Gallimore JF (1994) Detection of extended H I absorption toward PKS 2322–123 in Abell 2597. Astrophys J 436:669–677
Omar A, Dwarakanath KS, Rupen M, Anantharamaiah KR (2002) GMRT and VLA observations of H I and OH from the Seyfert galaxy Mrk 1. Astron Astrophys 394:405–414
Oort JH, Kerr FJ, Westerhout G (1958) Mon Not R Astron 118:379
Oosterloo TA, Morganti R, Tzioumis A, Reynolds J, King E, McCulloch P, Tsvetanov Z (2000) A strong jet-cloud interaction in the Seyfert galaxy IC 5063: VLBI observations. Astron J 119:2085–2091
Oosterloo T et al (2010) Early-type galaxies in different environments: an H I view. Mon Not R Astron Soc 409:500–514
Oosterloo T, Raymond Oonk JB, Morganti R, Combes F, Dasyra K, Salomé P, Vlahakis N, Tadhunter C (2017) Properties of the molecular gas in the fast outflow in the Seyfert galaxy IC 5063. Astron Astrophys 608:A38
Orienti M, Morganti R, Dallacasa D (2006) H I absorption in high-frequency peaker galaxies. Astron Astrophys 457:531–536
Ostorero L, Moderski R, Stawarz Ł, Diaferio A, Kowalska I, Cheung CC, Kataoka J, Begelman MC, Wagner SJ (2010) X-ray-emitting GHz-peaked-spectrum Galaxies: testing a dynamical-radiative model with broadband spectra. Astrophys J 715:1071–1093
Ostorero L, Morganti R, Diaferio A, Siemiginowska A, Stawarz Ł, Moderski R, Labiano A (2017) Correlation between X-ray and radio absorption in compact radio galaxies. Astrophys J 849:34
Padovani P (2016) The faint radio sky: radio astronomy becomes mainstream. Astron Astrophys Rev 24:13
Peck AB, Taylor GB, Conway JE (1999) Obscuration of the Parsec-scale jets in the compact symmetric object 1946+708. Astrophys J 521:103–111
Peck AB, Taylor GB (2001) Evidence for a circumnuclear Disk in 1946+708. Astrophys J 554:L147
Perlman ES, Stocke JT, Conway J, Reynolds C (2001) Host galaxies, obscuration, and nuclear structure of three nearby compact symmetric objects. Astron J 122:536–548
Pihlström YM, Vermeulen RC, Taylor GB, Conway JE (1999) H I absorption in the steep-spectrum superluminal quasar 3C 216. Astrophys J 525:L13–L16
Pihlström YM, Conway JE, Booth RS, Diamond PJ, Koribalski BS (2000) VLBA H I absorption observations of the water megamaser galaxy NGC 5793. Astron Astrophys 357:7–12
Pihlström YM, Conway JE, Vermeulen RC (2003) The presence and distribution of H I absorbing gas in sub-galactic sized radio sources. Astron Astrophys 404:871–881
Ramos Almeida C, Ricci C (2017) Nuclear obscuration in active galactic nuclei. Natu Astron 1:679–689
Richings AJ, Faucher-Giguère C-A (2018) The origin of fast molecular outflows in quasars: molecule formation in AGN-driven galactic winds. Mon Not R Astron Soc 474:3673–3699
Risaliti G, Woltjer L, Salvati M (2003) The nature of the absorbing torus in compact radio galaxies. Astron Astrophys 401:895–901
Roberts MS (1970) The detection of 21-centimeter hydrogen absorption arising from within the radio galaxy Centaurus a. Astrophys J 161:L9
Rodriguez C, Taylor GB, Zavala RT, Pihlström YM, Peck AB (2009) H I observations of the supermassive binary black hole system in 0402+379. Astrophys J 697:37–44

Rupke DS, Veilleux S, Sanders DB (2002) Keck absorption-line spectroscopy of galactic winds in ultraluminous infrared galaxies. Astrophys J 570:588–609
Rupke DS, Veilleux S, Sanders DB (2005) Outflows in infrared-luminous starbursts at $z<0.5$, I. sample, Na I D spectra, and profile fitting. Astrophys J Suppl Series 160:87–114
Rupke DSN, Veilleux S (2011) Integral field spectroscopy of massive, kiloparsec-scale outflows in the infrared-luminous QSO Mrk 231. Astrophys J 729:L27
Rupke DSN, Veilleux S (2013) The multiphase structure and power sources of galactic winds in major mergers. Astrophys J 768:75
Russell HR et al (2017) Close entrainment of massive molecular gas flows by radio bubbles in the central galaxy of Abell 1795. Mon Not R Astron Soc 472:4024–4037
Saikia DJ, Gupta N, Konar C (2007) H I gas in rejuvenated radio galaxies: Giant Metrewave Radio Telescope observations of the DDRG J1247+6723. Mon Not R Astron Soc 375:L31–L35
Salomé P, Combes F, Edge AC, Crawford C, Erlund M, Fabian AC, Hatch NA, Johnstone RM, Sanders JS, Wilman RJ (2006) Cold molecular gas in the Perseus cluster core. Association with X-ray cavity, Hα filaments and cooling flow. Astron Astrophys 454:437–445
Salter CJ, Saikia DJ, Minchin R, Ghosh T, Chandola Y (2010) The discovery of host galaxy H I absorption in CTA 21. Astrophys J 715:L117–L120
Sanders RH (2014) The dark matter problem, by Robert H. Cambridge University Press, Cambridge
Sancisi R, Fraternali F, Oosterloo T, van der Hulst T (2008) Astron Astrophys Rev 15:189
Santoro F (2018) The multi-phase ISM of radio galaxies: a spectroscopic study of ionized and warm gas. Doctor of Philosophy, University of Groningen. https://www.rug.nl/research/portal/en/publications/the-multiphase-ism-of-radio-galaxies-a-spectroscopic-study-of-ionized-and-warm-gas(494548fa-4e1e-45d6-85d2-4f54332418a4).html
Sarma AP, Troland TH, Rupen MP (2002) VLA H I Zeeman observations of Centaurus A. Astrophys J 564:696–703
Scannapieco E (2017) The production of cold gas within galaxy outflows. Astrophys J 837:28
Serra P et al (2012) The ATLAS^{3D} project - XIII. Mass and morphology of H I in early-type galaxies as a function of environment. Mon Not R Astron Soc 422:1835–1862
Shafi N, Oosterloo TA, Morganti R, Colafrancesco S, Booth R (2015) The 'shook up' galaxy NGC 3079: the complex interplay between H I, activity and environment. Mon Not R Astron Soc 454:1404–1415
Shostak GS, van Gorkom JH, Ekers RD, Sanders RH, Goss WM, Cornwell TJ (1983) A search for neutral hydrogen in radio galaxies. Astron Astrophys 119:L3–L6
Shulevski A et al (2015) The peculiar radio galaxy 4C 35.06: a case for recurrent AGN activity? Astron Astrophys 579:A27
Sijbring D, de Bruyn AG, Jaffe WJ, Sancisi R (1989) H I in the low velocity system of NGC1275. Eur South Observ Conf Workshop Proc 32:107
Srianand R, Gupta N, Momjian E, Vivek M (2015) Circumnuclear and infalling H I gas in a merging galaxy pair at $z = 0.123$. Mon Not R Astron Soc 451:917–926
Staveley-Smith L, Oosterloo T (2015) H I science with the square kilometre array. Adv Astrophys Square Kilometre Array (AASKA14) 167
Spitzer L (1978) Physical processes in the interstellar medium, by Lyman Spitzer. New York Wiley-Interscience, p 333
Stanghellini C, O'Dea CP, Dallacasa D, Cassaro P, Baum SA, Fanti R, Fanti C (2005) Extended emission around GPS radio sources. Astron Astrophys 443:891–902
Struve C, Oosterloo T, Sancisi R, Morganti R, Emonts BHC (2010a) Cold gas in massive early-type galaxies: the case of NGC 1167. Astron Astrophys 523:A75
Struve C, Oosterloo TA, Morganti R, Saripalli L (2010b) Centaurus A: morphology and kinematics of the atomic hydrogen. Astron Astrophys 515:A67
Struve C, Conway JE (2010) An H I absorbing circumnuclear disk in Cygnus A. Astron Astrophys 513:A10
Struve C, Conway JE (2012) The circumnuclear cold gas environments of the powerful radio galaxies 3C 236 and 4C 31.04. Astron Astrophys 546:A22
Tadhunter C (2008) The importance of sub-relativistic outflows in AGN host galaxies. Memorie della Societa Astronomica Italiana 79:1205
Tadhunter C, Morganti R, Rose M, Oonk JBR, Oosterloo T (2014) Jet acceleration of the fast molecular outflows in the Seyfert galaxy IC 5063. Nature 511:440–443
Tadhunter C (2016) Radio AGN in the local universe: unification, triggering and evolution. Astron Astrophys Rev 24:10

Taylor GB (1996) The symmetric parsec-scale jets of the radio galaxy Hydra A. Astrophys J 470:394
Taylor GB, O'Dea CP, Peck AB, Koekemoer AM (1999) H I absorption toward the nucleus of the radio galaxy PKS 2322–123 in A2597. Astrophys J 512:L27–L30
Taylor GB, Peck AB, Ulvestad JS, O'Dea CP (2004) Exploring the nucleus of the gigamaser galaxy TXS 2226–184. Astrophys J 612:780–785
Taylor GB, Peck AB, Henkel C, Falcke H, Mundell CG, O'Dea CP, Baum SA, Gallimore JF (2002) H I absorption in the gigamaser galaxy TXS 2226–184 and the relation between H I absorption and water emission. Astrophys J 574:88–94
Tengstrand O, Guainazzi M, Siemiginowska A, Fonseca Bonilla N, Labiano A, Worrall DM, Grandi P, Piconcelli E (2009) The X-ray view of giga-hertz peaked spectrum radio galaxies. Astron Astrophys 501:89–102
Teng SH, Veilleux S, Baker AJ (2013) Green Bank telescope detection of polarization-dependent H I absorption and H I outflows in local ULIRGs and Quasars. Astrophys J 765:95
Tingay SJ et al (2013) The Murchison widefield array: the square kilometre array precursor at low radio frequencies. Publ Astron Soc Austr 30:e007
Tremblay GR, O'Dea CP, Baum SA, Koekemoer AM, Sparks WB, de Bruyn G, Schoenmakers AP (2010) Episodic star formation coupled to reignition of radio activity in 3C 236. Astrophys J 715:172–185
Tremblay GR et al (2016) Cold, clumpy accretion onto an active supermassive black hole. Nature 534:218–221
Ursini F, Bassani L, Panessa F, Bazzano A, Bird AJ, Malizia A, Ubertini P (2018) Where are Compton-thick radio galaxies? A hard X-ray view of three candidates. Mon Not R Astron Soc 474:5684–5693
Uson JM, Bagri DS, Cornwell TJ (1991) Radio detections of neutral hydrogen at redshift $z = 3.4$. Phys Rev Lett 67:3328–3331
van Bemmel IM, Morganti R, Oosterloo T, van Moorsel G (2012) A relation between circumnuclear H I, dust, and optical cores in low-power radio galaxies. Astron Astrophys 548:A93
van Gorkom JH, Knapp GR, Ekers RD, Ekers DD, Laing RA, Polk KS (1989) H I absorption in radio elliptical galaxies: evidence for infall. Astron J 97:708–719
van Langevelde HJ, Pihlström YM, Conway JE, Jaffe W, Schilizzi RT (2000) A thin H I circumnuclear disk in NGC 4261. Astron Astrophys 354:L45–L48
Verheijen M, van Gorkom JH, Szomoru A, Dwarakanath KS, Poggianti BM, Schiminovich D (2007) WSRT ultradeep neutral hydrogen imaging of galaxy clusters at $z \sim 0.2$: a pilot survey of Abell 963 and Abell 2192. Astrophys J 668:L9–L13
Vermeulen RC et al (2003a) Observations of H I absorbing gas in compact radio sources at cosmological redshifts. Astron Astrophys 404:861–870
Vermeulen RC, Ros E, Kellermann KI, Cohen MH, Zensus JA, van Langevelde HJ (2003) The shroud around the twin radio jets in NGC 1052. Astron Astrophys 401:113–127
Vermeulen RC, Labiano A, Barthel PD, Baum SA, de Vries WH, O'Dea CP (2006) Atomic hydrogen in the one-sided "compact double" radio galaxy 2050+364. Astron Astrophys 447:489–498
Véron-Cetty M-P, Woltjer L, Staveley-Smith L, Ekers RD (2000) The nature of powerful compact radio galaxies. Astron Astrophys 362:426–434
Verschuur GL, Kellermann KI (1988) Galactic and extra-galactic radio astronomy, 2nd ed., edited by Verschuur, Gerrit L.; Kellermann, Kenneth I. Springer, Berlin
Vink J, Snellen I, Mack K-H, Schilizzi R (2006) The X-ray properties of young radio-loud AGN. Mon Not R Astron Soc 367:928–936
Wagner AY, Bicknell GV (2011) Relativistic jet feedback in evolving galaxies. Astrophys J 728:29
Wagner AY, Bicknell GV, Umemura M (2012) Driving outflows with relativistic jets and the dependence of active galactic nucleus feedback efficiency on interstellar medium inhomogeneity. Astrophys J 757:136
Whiteoak JB, Gardner FF (1976) H I absorption in NGC 4945. Proc Astron Soc Aust 3:71
Wilman RJ, Miller L, Jarvis MJ et al (2008) A semi-empirical simulation of the extragalactic radio continuum sky for next generation radio telescopes. Mon Not R Astron Soc 388:1335
Wilms J, Allen A, McCray R (2000) On the absorption of X-rays in the interstellar medium. Astrophys J 542:914
Wilson TL, Rohlfs K (2013) Hüttemeister S (2013) tools of radio astronomy. Astron Astrophys Library. Springer, Berlin
Wolfire MG (2010) Highlights Astron 15:409

Yan T, Stocke JT, Darling J, Momjian E, Sharma S, Kanekar N (2016) Invisible active galactic nuclei. II. Radio morphologies and five new H I 21cm absorption line detectors. Astron J 151:74
Zubovas K, King A (2012) Clearing out a galaxy. Astrophys J 745:L34

Affiliations

Raffaella Morganti[1,2] · Tom Oosterloo[1,2]

✉ Raffaella Morganti
morganti@astron.nl

Tom Oosterloo
oosterloo@astron.nl

1 ASTRON, The Netherlands Institute for Radio Astronomy, Postbus 2, 7990 AA Dwingeloo, The Netherlands

2 Kapteyn Astronomical Institute, University of Groningen, Postbus 800, 9700 AV Groningen, The Netherlands